Genetics and Genomics
Neuroscience

Acute avoidance of hydrogen sulfide is modulated by external and internal states in *C. elegans*

Reviewed Preprint

Published from the original preprint after peer review and assessment by eLife.

About eLife's process

Reviewed preprint version 1
December 27, 2023 (this version)

Posted to preprint server
October 13, 2023

Sent for peer review
October 9, 2023

Longjun Pu, Lina Zhao, Jing Wang, Johan Henriksson, Patrick Laurent, Changchun Chen

Department of Molecular Biology, Umeå University, Umeå, Sweden • Umeå Centre for Molecular Medicine, Umeå University, Umeå, Sweden • Wallenberg Centre for Molecular Medicine, Umeå University, Umeå, Sweden • The Laboratory for Molecular Infection Medicine Sweden (MIMS), Umeå University, Umeå, Sweden • Integrated Science Lab (Icelab), Umeå University, Umeå, Sweden • Laboratory of Neurophysiology, ULB Neuroscience Institute (UNI), Université Libre de Bruxelles (ULB), Belgium

Abstract

Hydrogen sulfide (H_2S) can act as an energy source, a poison and a gasotransmitter in organisms. We used the robust locomotory responses to H_2S in *Caenorhabditis elegans* to delineate the molecular mechanisms governing sensory and adaptive responses to H_2S exposure. We found that *C. elegans* exhibited transiently increased locomotory activity and turning behavior as a strategy to escape the noxious H_2S stimulation. The behavioral responses to H_2S were modulated by a complex network of signaling pathways, including cyclic GMP signaling in ciliated sensory neurons, calcineurin, nuclear hormone receptors, to the major starvation regulators such as insulin and TGF-β signaling. The response to H_2S was substantially affected by the ambient O_2 levels and their prior experience in low O_2 environments, suggesting an intricate interplay between O_2 and H_2S sensing mechanisms. Prolonged exposure to H_2S robustly evoked H_2S detoxification coupled with reduced locomotory response to the subsequent H_2S challenges. Intriguingly, the expression of genes involved in iron homeostasis, including *ftn-1* and *smf-3*, was substantially modified in exposure to H_2S, implying that labile iron levels are affected by H_2S. In support of this, iron supplement significantly bolstered the behavioral response to H_2S. In addition, mitochondria, one of the central hubs for H_2S metabolism, played a crucial role in adaptive responses to H_2S. In summary, our study provides molecular insights into the mechanisms through which *C. elegans* detects, modulates, and adapts its response to H_2S.

eLife assessment

The manuscript aims to better understand the mechanisms underlying the behavioral responses of C. elegans to hydrogen sulfide, a toxin known to exert remarkable effects on animal physiology in a range of contexts. To this end, the authors provide a series of **useful** findings regarding the mechanisms by which hydrogen sulfide may be sensed, their relationships to other gas-sensing pathways, and the role of a variety of physiological pathways in responding to hydrogen sulfide exposure. While some of the findings are **solid**, other aspects of the paper are **incomplete**, such that some claims are **incompletely** supported, and an integrated understanding of the authors' observations does not clearly emerge.

Introduction

The detection and response to chemical signals are crucial to interact effectively with the environment in various organisms, spanning from bacteria to humans. During the late Proterozoic era, the rise in oxygen (O_2) levels eliminated hydrogen sulfide (H_2S) from most of the habitats. Yet, low O_2 levels together with high concentrations of H_2S and carbon dioxide (CO_2) can still persist in enclosed environments where bacteria actively decompose organic matter (Olson & Straub, 2016). H_2S can easily penetrate biological membranes and interfere with various cellular processes, leading to toxicity. One of its detrimental effects is the disruption of cellular respiration by binding to cytochrome c oxidase (COX) and inhibiting the mitochondrial electron transport chain (Cooper & Brown, 2008; Khan et al., 1990; Nicholls & Kim, 1982b).

Animals inhabiting environments rich in H_2S have evolved mechanisms to either avoid or adapt to high concentrations of H_2S, providing them with survival advantages. Species that encounter periodic increases in H_2S often possess sensing abilities and exhibit avoidance behaviors. For example, benthic species undertake daily vertical migrations between sulfidic and non-sulfidic waters (Abel, Koenig, & Davis, 1987; Salvanes, Utne-Palm, Currie, & Braithwaite, 2011). Certain metazoan species have seized the ecological opportunities presented by H_2S-rich environments through the development of cellular adaptations, allowing them to occupy a unique ecological niche that is inaccessible to the other organisms. Livebearing fish species, for instance, have evolved COX subunits that are more resistant to H_2S and are more efficient in H_2S detoxification (Kelley et al., 2016; Pfenninger et al., 2014).

Free living nematodes thrive in decaying matter where they are exposed to significant fluctuations in O_2, CO_2, and H_2S levels over short distances (Rodriguez-Kabana, Jordan, & Hollis, 1965). Nematodes like *C. elegans* have evolved the ability to utilize these gasous stimuli to navigate their environment, locate bacterial food sources, or escape the dangers (Bretscher, Busch, & de Bono, 2008; Carrillo, Guillermin, Rengarajan, Okubo, & Hallem, 2013). Acute exposure to H_2S triggers transiently increased locomotion in *C. elegans* (Budde & Roth, 2011). However, prolonged exposure to H_2S induces cellular adaptation to survive the toxic environment. *C. elegans* can tolerate H_2S levels up to 50 ppm, but the concentrations exceeding 150 ppm prove lethal (Budde & Roth, 2010, 2011; Fawcett, Hoyt, Johnson, & Miller, 2015; Horsman, Heinis, & Miller, 2019; Miller, Budde, & Roth, 2011a; Miller & Roth, 2007). Extended periods of low O_2 and/or high H_2S exposure stabilize the hypoxia-inducible factor HIF-1, leading to transcriptional reprogramming (Budde & Roth, 2010). Through HIF-1-dependent and independent mechanisms, acclimation of *C. elegans* to 50 ppm H_2S extends lifespan and improves the response to hypoxia-induced protein aggregation (Budde & Roth, 2010; Fawcett et al., 2015; Horsman et al., 2019; Miller & Roth, 2007; Qabazard et al., 2014).

In this study, we investigated how the nematode *C. elegans* responds acutely to avoid an increase of H_2S levels, as well as how it adapts at the molecular and physiological levels if they fail to escape the H_2S exposure.

Results

cGMP signaling in ASJ cilia contributes to H_2S avoidance

When encountering aversive cues such as noxious gases, *C. elegans* initiates a pirouette followed by an increase of its locomotory activity to escape the noxious stimuli. When acutely exposed to 150 ppm H_2S, *C. elegans* exhibited an increased locomotory speed and enhanced turning behavior, while decreasing the frequency of reversals, as a strategy to escape the noxious stimuli (***Figure 1—figure supplement 1A–C***). The maximum speed was reached after 6–8 minutes in H_2S, and returned to the baseline over a period of approximately 1 hour (***Figure 1—figure supplement 1D***). The reduced locomotory activity after 2 hours in H_2S was fully reversible if these animals were immediately challenged by a different stimulus such as hypoxia (***Figure 1—figure supplement 1E***). The magnitude of the avoidance responses appeared to be concentration dependent. Under our assay conditions, acute behavioral response to 50 ppm H_2S was minimal and lacked consistency, whereas the response to 150 ppm H_2S was robust and reproducible (***Figure 1—figure supplement 1F***).

To gain molecular insight into H_2S evoked locomotory response, we performed a candidate screen for mutants that failed to increase their locomotory speed when H_2S levels acutely increased to 150 ppm (***Supplementary file 1***). We discovered that mutants defective in ciliogenesis exhibited diminished H_2S responses (***Figure 1A–C***). These included *daf-19* mutants lacking cilia, *dyf-3* mutants with reduced cilia length, and *dyf-7* mutants where ciliogenesis occurs but the cilia are not anchored to their sensilla and are not exposed to the external environment (Heiman & Shaham, 2009; Murayama, Toh, Ohshima, & Koga, 2005; Starich et al., 1995; Swoboda, Adler, & Thomas, 2000). Our observations suggest that cilia exposure to the external environment is necessary for H_2S detection. Cilia-mediated sensory responses often involve the activation of guanylate cyclases and the opening of cGMP-gated channels (Ferkey, Sengupta, & L'Etoile, 2021). We observed attenuated H_2S responses in *tax-4* or *tax-2* mutants, lacking the key subunits of cilia-enriched cGMP-gated channels (***Figure 1D and E***). Comparable observations have also been reported in acute response to CO_2, suggesting that locomotory responses to CO_2 and H_2S are similar (Bretscher et al., 2008; Hallem et al., 2011; Hallem & Sternberg, 2008). Consistent with this, mutations in genes encoding the calcineurin subunits TAX-6 or CNB-1, or nuclear hormone receptor NHR-49, impaired both H_2S and CO_2 responses (Hallem & Sternberg, 2008) (***Figure 1—figure supplement 2A–C***). Additionally, locomotory response to H_2S was also repressed following a 24-hour period of starvation, as observed for CO_2 (***Figure 1—figure supplement 2D***) (Bretscher et al., 2008; Hallem & Sternberg, 2008). In *C. elegans*, the regulation of starvation-responses involves the reduced activity of two major pathways: insulin and TGF-β signaling. Disrupting the genes encoding the insulin receptor DAF-2 or the TGF-β ligand DAF-7 eliminated locomotory activity in response to acute H_2S (***Figure 1F and G***, ***Figure 1—figure supplement 2E***). Insulin and TGF-β signaling involve the inhibition of downstream transcription factors DAF-16 or DAF-3 respectively. H_2S avoidance defects of *daf-2* and *daf-7* mutants were fully suppressed in *daf-2; daf-16* or in *daf-7; daf-3* double mutants (***Figure 1F and G***).

These observations prompted us to further investigate if the same molecular and circuit mechanisms underlay the acute avoidance to CO_2 and H_2S. The response to CO_2 requires receptor guanylate cyclase GCY-9 (Hallem et al., 2011). Interestingly, GCY-9 was dispensable for the locomotory responses to H_2S (***Figure 1H***). In addition, animals responded more rapidly to CO_2 than to H_2S, but with a reduced magnitude (***Figure 1I***), implying that distinct mechanisms likely

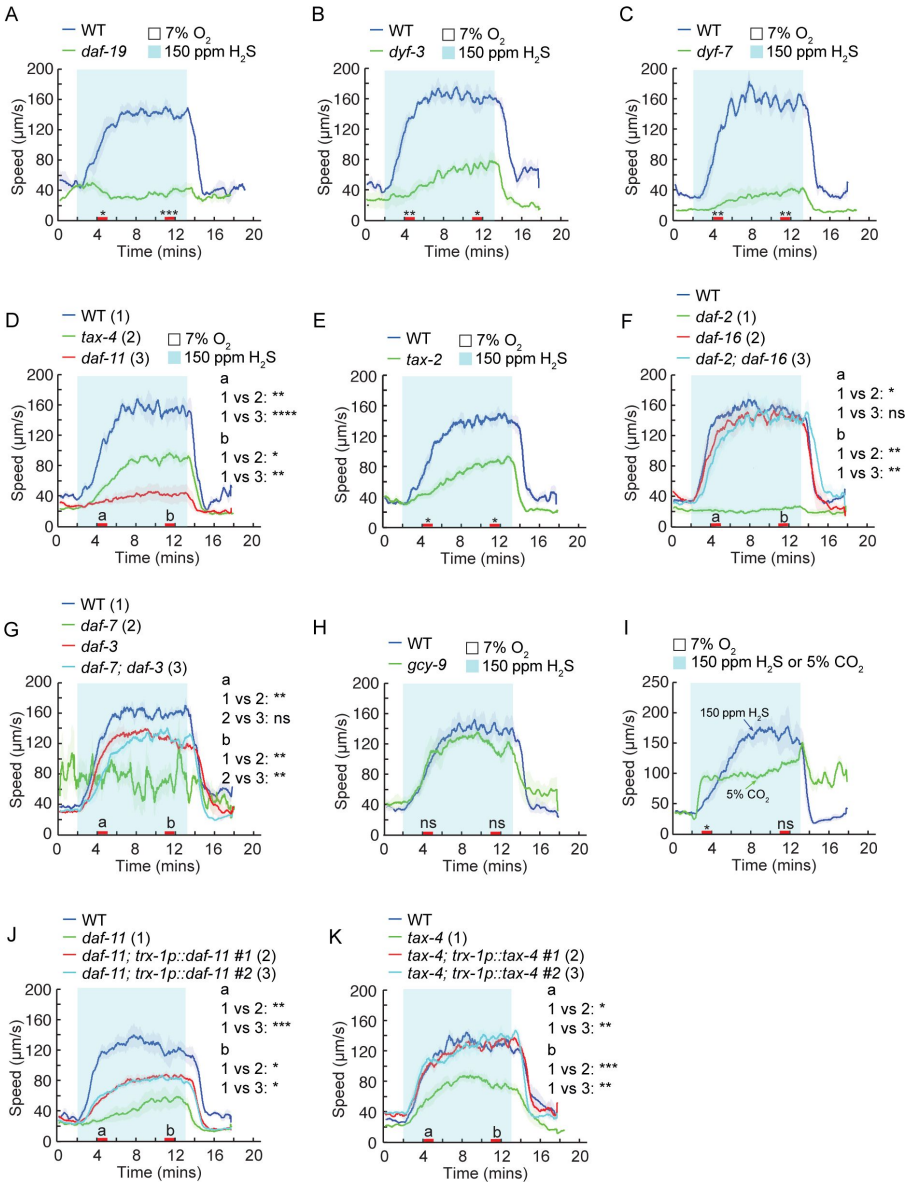

Figure 1.

cGMP signaling in ASJ neurons contributes to H_2S avoidance

(**A–H**) Locomotory responses to a switch from 7% O_2 to 150 ppm H_2S balanced with 7% O_2 for animals of the indicated genotype: WT (N2) and *daf-19(m86)* (**A**); WT and *dyf-3(m185)* (**B**); WT and *dyf-7(m539)* (**C**); WT, *daf-11(m47)* and *tax-4(p678)* (**D**); WT and *tax-2(p691)* (**E**); WT, *daf-2(e1370), daf-16(mgDf47) and daf-2(e1370); daf-16(mgDf47) double mutants* (**F**); WT, *daf-7(e1372), daf-3(mgDf90) and daf-7(e1372); daf-3(mgDf90) double mutants* (**G**); WT and *gcy-9(tm7632)* (**H**). In this and subsequent figures for H_2S assay, red bars on the x-axis represent two intervals (4–5 minutes and 11–12 minutes, labeled as a and b respectively in **Figure 1D**, F, G, J and K) used for statistical analysis unless otherwise indicated. **** = $p < 0.0001$, *** = $p < 0.001$, ** = $p < 0.01$, * = $p < 0.05$, ns = not significant, Mann–Whitney U test. (**I**) Comparison between the acute locomotory response of WT animals to 150 ppm H_2S balanced with 7% O_2 and the acute locomotory response to 5% CO_2 balanced with 7% O_2. Red bars on the x-axis indicate two intervals (3-4 minutes and 11-12 minutes) used for statistical analysis. * = $p < 0.05$, ns = not significant, Mann–Whitney U test. (**J**) Locomotory responses to a switch from 7% O_2 to 150 ppm H_2S balanced with 7% O_2 for animals of the indicated genotype: WT, *daf-11(m47)* and transgenic *daf-11(m47)* expressing *daf-11* genomic DNA in ASJ neurons (two independent lines). *** = $p < 0.001$, ** = $p < 0.01$, * = $p < 0.05$, Mann–Whitney U test. (**K**) Locomotory responses to a switch from 7% O_2 to 150 ppm H_2S balanced with 7% O_2 for animals of the indicated genotype: WT, *tax-4(p678)* and transgenic *tax-4(p678)* expressing *tax-4* cDNA in ASJ neurons (two independent lines). *** = $p < 0.001$, ** = $p < 0.01$, * = $p < 0.05$, Mann–Whitney U test.

drive these two responses. In a comprehensive survey of all guanylate cyclase mutants, the *daf-11* strain emerged as the only mutant showing defects in the avoidance of H_2S (***Figure 1D, Supplementary file 1***). Selective expression of *daf-11* in ASJ neurons, but not in other neurons, partially restored the locomotory response to acute H_2S (***Figures 1J***, ***Figure 1—figure supplement 2F–I***). Consistently, the H_2S response defect of *tax-4* mutants was also rescued by selective expression of its cDNA in ASJ neurons (***Figure 1K***), suggesting that the receptor guanylate cyclase DAF-11 and the CNG channel TAX-4 partially act in ASJ neurons to promote acute response to H_2S. This differed from the site of action of the CO_2 sensor GCY-9, which primarily operates in BAG neurons (Hallem et al., 2011). Taken together, these observations suggest that common signaling pathways modulate the locomotory responses to both H_2S and CO_2, although the molecular and circuit underpinning of H_2S and CO_2 sensing are different.

Activation of the O_2 sensing circuit antagonizes H_2S avoidance

The sensory responses of wild *C. elegans* are adapted to their living environment, which is characterized by low O_2 levels and high concentrations of CO_2. In comparison to the domesticated lab strain N2, wild isolates of *C. elegans* exhibit a strong response to high O_2 but are relatively indifferent to CO_2 (Beets et al., 2020; Bretscher et al., 2008; Hallem & Sternberg, 2008). Local H_2S concentrations could also be significantly higher in decomposing substances where wild *C. elegans* thrives. We suspected that wild strains could display a modified response to H_2S in comparison to standard laboratory N2 animals. Indeed, wild isolates CB4855, CB4856, and CB4858 exhibited attenuated responses to H_2S (***Figure 2A***, ***Figure 2—figure supplement 1A***). One predominant genetic trait in these strains is a naturally occurring variation of neuropeptide receptor NPR-1 215F, which is less active than NPR-1 215V in N2 animals (de Bono & Bargmann, 1998). This led us to investigate whether the NPR-1 signaling plays a role in modulating acute avoidance of H_2S. Mutating *npr-1* in N2 strain background was sufficient to abolish locomotory responses to H_2S, as observed in the wild isolates (***Figure 2B***). NPR-1 primarily acts within the RMG interneurons to modulate responses to environmental stimuli by reducing signal output from these neurons (Laurent et al., 2015; Macosko et al., 2009). The selective expression of the highly active *npr-1(215V)* variant in RMG neurons effectively restored H_2S evoked locomotory response in *npr-1* mutant worms (***Figure 2C***). Furthermore, optogenetic stimulation of RMG interneurons using channelrhodopsin-2 (ChR2) significantly dampened locomotory response to H_2S of N2 animals, suggesting high RMG activity inhibits H_2S responses (***Figure 2—figure supplement 1B***).

The sensation of 21% O_2 involves the soluble guanylate cyclases GCY-35/GCY-36 and the downstream cyclic nucleotide gated (CNG) channels TAX-4/TAX-2 (Busch et al., 2012; Cheung, Cohen, Rogers, Albayram, & de Bono, 2005; Couto, Oda, Nikolaev, Soltesz, & de Bono, 2013; Gray et al., 2004; Laurent et al., 2015; Persson et al., 2009; Zimmer et al., 2009). We examined if disrupting O_2 sensing machinery had the same effect as the inhibition of RMG signaling by NPR-1(215V). We found that silencing O_2 sensing neurons by mutating *gcy-35* and *tax-4*, or ablating these neurons by cell-specific expression of the pro-apoptotic gene *egl-1* restored H_2S evoked behavioral response in *npr-1* null mutants (***Figure 2D–F***). Specific expression of *gcy-35* cDNA in URX, AQR, PQR was sufficient to repress acute response to H_2S in *npr-1; gcy-35* double mutants (***Figure 2G***). Finally, enhancing the presynaptic activities of URX, AQR, PQR neurons by the expression of a gain-of-function PKC-1(A160E) (Dekker, Mcintyre, & Parker, 1993; Hiroki et al., 2022) significantly dampened H_2S regulated locomotory activity (***Figure 2—figure supplement 1C***). Taken together, these observations indicate that activation of O_2 sensing circuit is inhibitory to H_2S evoked locomotory response.

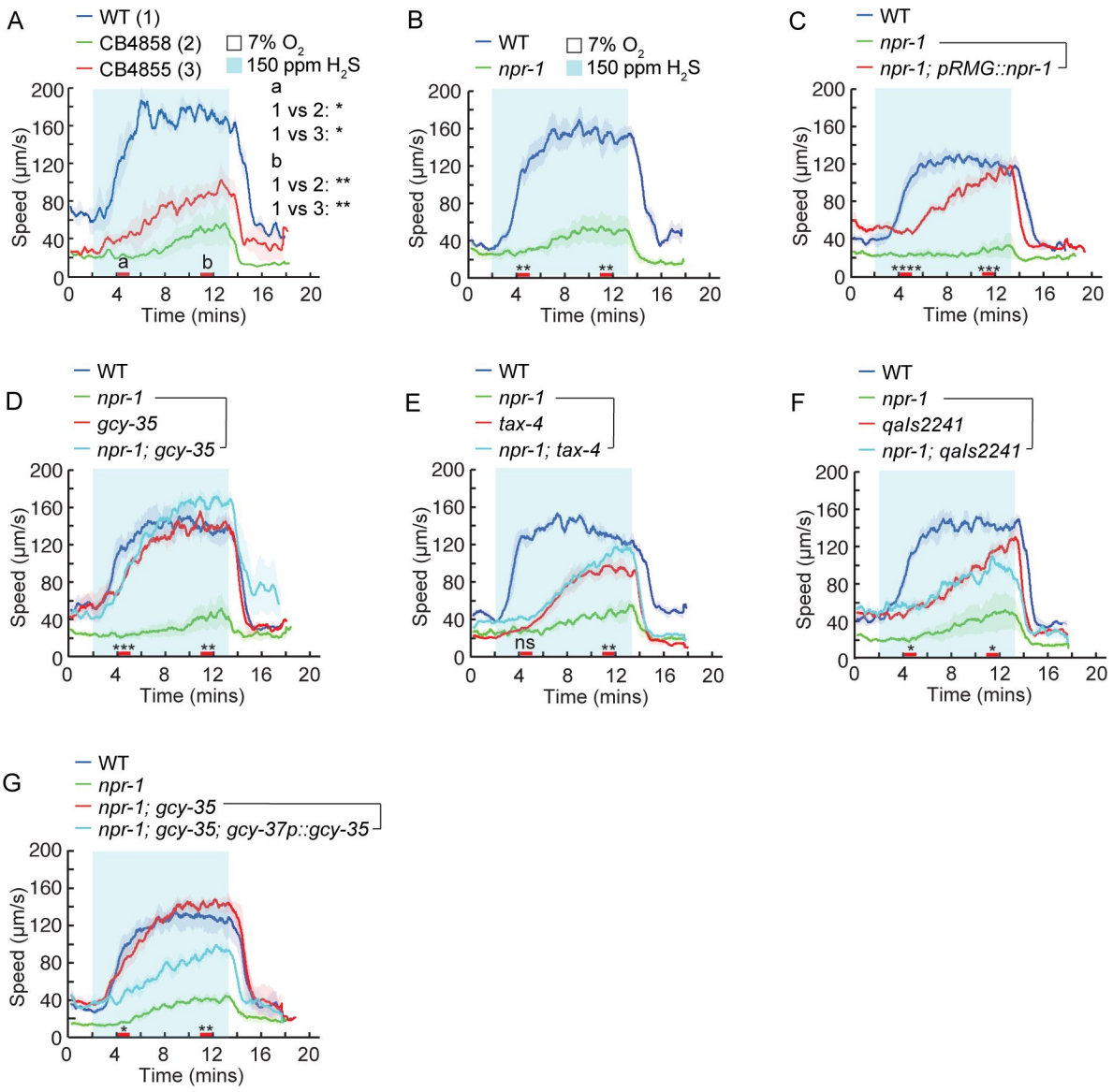

Figure 2.

Activation of O_2 sensing circuit antagonizes H_2S avoidance

(**A**) Locomotory responses to a switch from 7% O_2 to 150 ppm H_2S balanced with 7% O_2 for WT animals, wild isolates CB4858 and CB4855. Red bars on the x-axis represent two intervals (4–5 minutes and 11–12 minutes, labeled as a and b respectively), used for statistical analyses. ** = $p < 0.01$, * = $p < 0.05$, Mann–Whitney U test. (**B, C**) Locomotory responses to a switch from 7% O_2 to 150 ppm H_2S balanced with 7% O_2 for animals of the indicated genotype: WT and *npr-1(ad609)* (**B**); WT, *npr-1(ad609) and* transgenic *npr-1(ad609)* expressing *npr-1* in RMG neurons using Cre-LoxP system (Macosko et al., 2009) (**C**). Red bars on the x-axis indicate two intervals (4-5 minutes and 11-12 minutes) used for statistical analysis. **** = $p < 0.0001$, *** = $p < 0.001$, ** = $p < 0.01$, Mann–Whitney U test. (**D–G**) Locomotory responses to a switch from 7% O_2 to 150 ppm H_2S balanced with 7% O_2 for animals of the indicated genotype: WT, *npr-1(ad609), gcy-35(ok769)* and *npr-1(ad609); gcy-35(ok769)* double mutants (**D**); WT, *npr-1(ad609), tax-4(p678)* and *npr-1(ad609); tax-4(p678)* double mutants (**E**); WT, *npr-1(ad609), qaIs2241*(genetic ablation of AQR, PQR and URX neurons) and *npr-1(ad609); qaIs 2241* (**F**); WT, *npr-1(ad609), npr-1(ad609); gcy-35(ok769)* double mutants and *transgenic npr-1(ad609); gcy-35(ok769)* double mutants expressing *gcy-35* cDNA under *gcy-37* promoter, which drives expression in O_2 sensing neurons (**G**). Red bars on the x-axis indicate two intervals (4-5 minutes and 11-12 minutes) used for statistical analysis. *** = $p < 0.001$, ** = $p < 0.01$, * = $p < 0.05$, ns = not significant, Mann–Whitney U test.

H_2S exposure reprograms gene expression in *C. elegans*

Prolonged exposure to H_2S has a dramatic impact on the physiology of *C. elegans*: 50 ppm H_2S exposure extends its lifespan, while 150 ppm H_2S is lethal (Budde & Roth, 2010, 2011; Fawcett et al., 2015; Horsman et al., 2019; Miller & Roth, 2007 Miller, 2011 #5). We conducted a comparative analysis of the transcriptome profiles in animals exposed to either 50 ppm or 150 ppm H_2S for the durations of 1 hour, 2 hours, or 12 hours. Our RNA-seq analysis revealed that a one-hour exposure to either 50 ppm or 150 ppm H_2S was sufficient to trigger significant changes in gene expression, with 518 or 304 genes showing differential expression, respectively (***Figure 3A**, **Supplementary file 2, p<1e-10***). Genes induced by 1-hour and 2-hour H_2S exposure displayed a considerable overlap (***Figure 3B**, **Figure 3— figure supplement 1A***). Gene Ontology (GO) analysis revealed that biological processes such as defense against bacteria and cysteine biosynthesis from L-serine were immediately activated upon H_2S exposure (***Figure 3C** **and D**, **Figure 3—figure supplement 1B** **and C***). As expected, we observed a robust induction of genes involved in H_2S detoxification (***Figure 3E** **and F***) (Miller, Budde, & Roth, 2011b; Niu et al., 2011; Vora et al., 2022). H_2S is detoxified in mitochondria by sulfide:quinone oxidoreductase SQRD-1 to persulfide, which is then metabolized by sulfur dioxygenase ETHE-1 to generate sulfite. Thiosulfate transferase further oxidizes sulfite to produce thiosulfate (Hildebrandt & Grieshaber, 2008). Glutathione S-transferases (GSTs) remove accumulated sulfur molecules during H_2S oxidation (Jackson, Melideo, & Jorns, 2012). Notably, *gst-19* and *sqrd-1* were among the most significantly upregulated genes after one or two hours of exposure to either 50 ppm or 150 ppm H_2S, while *ethe-1* showed a weak increase (***Figure 3E** **and F**, **Figure 3—figure supplement 1D** **and E**, **Supplementary file 2***). H_2S activates the HIF-1 pathway through the interaction of sulhydrylase/cysteine synthase CYSL-1 with the HIF-1 proline hydroxylase EGL-9 (Ma, Vozdek, Bhatla, & Horvitz, 2012). We found that a proportion of genes with HIF-1 regulated promoters displayed increased expression after 1 or 2 hours of H_2S exposure (***Figure 3— figure supplement 1F***) (Miller et al., 2011b; Vora et al., 2022). These genes included the above-mentioned detoxifying enzymes GST-19, SQRD-1, and ETHE-1, as well as enzymes involved in cysteine metabolism, CYSL-1, CYSL-2, and CDO-1 (***Supplementary file 2***). Mutations increasing SKN-1 activity bypass the requirement for HIF-1 to survive in high H_2S (Horsman et al., 2019). Consistent with early observations (Miller et al., 2011a), we also observed that a set of SKN-1 targets were differentially expressed in H_2S (***Figure 3—figure supplement 1G***) (Niu et al., 2011). This included the heat shock protein encoding genes *hsp-16.2* and *hsp-16.41* (***Figure 3E** **and F**, **Figure 3—figure supplement 1D** **and E***).

Surprisingly, we also observed a rapid increase in the expression of genes associated with intracellular H_2S production, such as *semo-1* and *mpst-3* genes (***Figure 3E** **and F**, **Figure 3—figure supplement 1D** **and E***) (Philipp et al., 2022; Qabazard et al., 2014). However, these data aligned with earlier observations made in sulfide spring fish (Kelley et al., 2016; Mathew, Schlipalius, & Ebert, 2011; Qabazard et al., 2014).

When exposed to the H_2S for 12 hours, the differentially expressed genes showed reduced overlap with those identified at earlier time points (***Figure 3B**, **Figure 3—figure supplement 1A***). This suggests that different defense strategies against H_2S might be employed at various stages of exposure. Although similar sets of genes were induced after 1h or 2h at 50 ppm and 150 ppm H_2S, the overlap between 50ppm and 150ppm decreased after 12 hours exposure (***Figure 3—figure supplement 1H–J***). This observation suggests that defense mechanisms might also differ for prolonged exposure at low and high levels of H_2S. In particular, we noted that 150 ppm H_2S specifically triggered the expression of the HIF-1 regulator *rhy-1* and the HIF-1 target *nhr-57* at all exposure time points, which was less pronounced in response to 50 ppm H_2S (***Figures 3E** **and F**, **Figure 3—figure supplement 1D, E, K** **and L***).

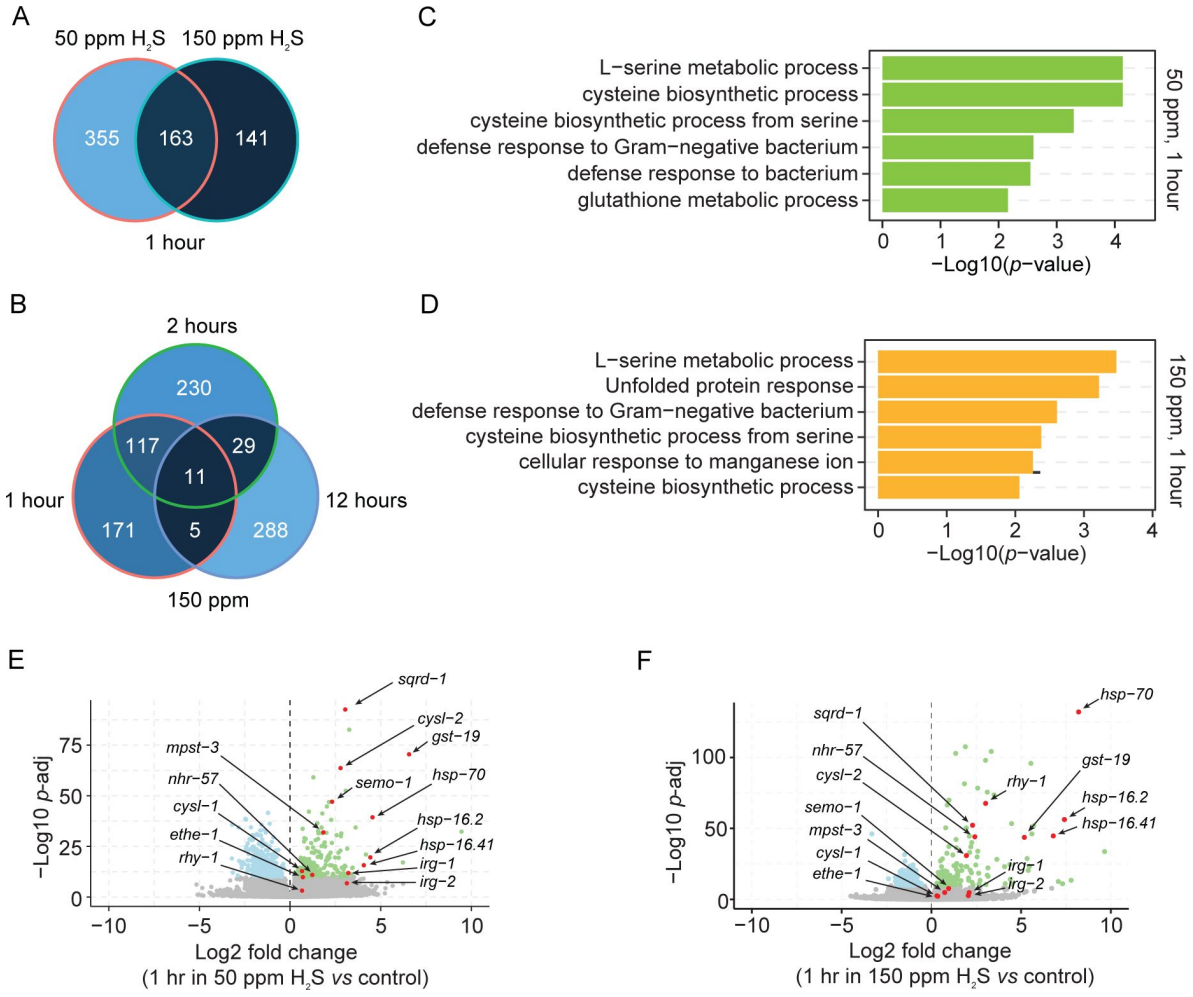

Figure 3.

Prolonged H_2S exposure reprograms gene expression in *C. elegans*

(**A**) Venn diagram displaying the number of differentially expressed genes after 1-hour exposure to 50 ppm or 150 ppm H_2S balanced with 7% O_2 in WT animals. p<1e-10. (**B**) Venn diagram displaying the number of differentially expressed genes after 1-hour, 2-hour and 12-hour exposure to 150 ppm H_2S balanced with 7% O_2 in WT animals. p<1e-10. (**C, D**) Significantly enriched GO categories for differentially expressed genes with adjusted p value <1e-10 in WT animals exposed to 50 ppm (**C**) or 150 ppm (**D**) H_2S balanced with 7% O_2 for 1 hour. (**E, F**) Volcano plots showing the differentially expressed genes with adjusted p value <1e-10 in WT animals exposed to 50 ppm (**E**) or 150 ppm (**F**) H_2S balanced with 7% O_2 for 1 hour. A set of genes involved in H_2S detoxification, cysteine metabolism and stress response were highlighted in red.

Acute response to H_2S is modulated by HIF-1 signaling

Consistent with early observations (Budde & Roth, 2010), our RNA-seq data suggested that H_2S exposure activates HIF-1 pathway (***Figure 3—figure supplement 1F***). Stabilization of HIF-1 by H_2S is critical for animals to survive H_2S exposure by the induction of detoxification genes as well as other adaptative responses (Ma et al., 2012). Such an adaptation is usually accompanied with the reduction in sensory sensitivity to this stressor. Therefore, we suspected that HIF-1 stabilization might dampen the acute response to H_2S. Under normoxia conditions, the conserved proline-4-hydroxylase PHD/EGL-9 hydroxylates HIF-1, which is subsequently recognized by the von Hippel-Lindau (VHL) tumor suppressor protein for degradation (Kaelin & Ratcliffe, 2008; Semenza, 2010). We found that disrupting *hif-1* resulted in extremely transient behavioral response to H_2S characterized by an initial bout of activity and a rapid decline of locomotory speed to the basal level (***Figure 4A***). While eliminating PHD/EGL-9 or VHL activity, which stabilizes HIF-1, the locomotory response to H_2S was completely inhibited (***Figure 4B***). *egl-9; hif-1* or *vhl-1; hif-1* double mutants had the identical response as *hif-1* mutants (***Figure 4C and D***), confirming that mutating *egl-9* or *vhl-1* inhibits acute response to H_2S by activating HIF-1. Acclimating animals in 1% O_2 for more than 12 hours also significantly decreased acute response to H_2S (***Figure 4E***). In addition, animals carrying the non-degradable form of HIF-1 in all neurons were defective in H_2S evoked locomotory responses (***Figure 4F***). Taken together, these observations suggest that constitutive activation of HIF-1 promotes the adaption to H_2S and inhibits the behavioral responses to H_2S stimulation.

The transient behavioral response to H_2S in *hif-1* mutants suggested that animals deficient of HIF-1 can still detect the presence of H_2S. This observation together with the importance of HIF-1 signaling in H_2S detoxification provoked us to explore whether detoxification enzymes were also required for the sustained locomotory activity in H_2S. Similar to *hif-1* mutants, both *sqrd-1* and *ethe-1* mutants displayed a transient response to H_2S (***Figure 4G and H***). We next examined the contribution of other upregulated genes in response to H_2S, including the genes encoding sulfhydrylase/cysteine synthases CYSL-1, CYSL-2, and CYSL-3 as well as SEMO-1. Disrupting CYSLs and SEMO-1 encoding genes phenocopied *hif-1* or *sqrd-1* mutants (***Figure 4I and J***). Our data suggest that while H_2S detoxification system is not essential for H_2S sensing, it is required for preserving animals' locomotory activity in the presence of H_2S.

Labile iron pool is critical to sustain the locomotory activity in H_2S

C. elegans tightly regulates iron homeostasis through the control of iron transporter SMF-3, as well as the regulation of iron storage protein Ferritins FTN-1 and FTN-2 (Cha'on et al., 2007; Gourley, Parker, Jones, Zumbrennen, & Leibold, 2003; Kim, Cho, Yoo, & Ahnn, 2004; Pekec et al., 2022). Among the most differentially regulated genes, *ftn-1* appeared to be consistently downregulated by H_2S (***Figure 5A and B, Figure 5—figure supplement 1A–D***). The inhibited expression of *ftn-1* and *ftn-2* as well as the elevated expression of *smf-3* (***Figure 5A and B, Figure 5—figure supplement 1A–D***) prompted us to explore if labile iron levels play a role in behavioral response to H_2S exposure. The labile iron pool is chelatable and redox-active. In the presence of iron chelator 2,2'-dipyridyl (BP), H_2S evoked locomotory response was fully inhibited (***Figure 5C***). This was not caused by the general sickness of BP-exposed animals as they responded robustly to acute hypoxia (***Figure 5—figure supplement 1E***). By contrast, the supplementation of ferric ammonium citrate (FAC) significantly prolonged animals' locomotory activity in H_2S (***Figure 5C***). In addition, disrupting *ftn-1*, which was expected to increase labile iron levels (Anderson & Leibold, 2014; Romney, Newman, Thacker, & Leibold, 2011), promoted the locomotory activity of animals in H_2S (***Figure 5D***), Conversely, mutating *smf-3*, which impaired iron uptake (Anderson & Leibold, 2014; Romney et al., 2011), led to a faster decline of locomotory activity in H_2S (***Figure 5D***). Furthermore, depleting labile iron pool by *ftn-1* overexpression resulted in an attenuated response to H_2S (***Figure 5E***), while it did not affect acute response to hypoxia (***Figure 5—figure supplement 1F***). These data suggests that high levels of free iron sustain locomotory activity in H_2S, whereas low iron levels inhibit behavioral

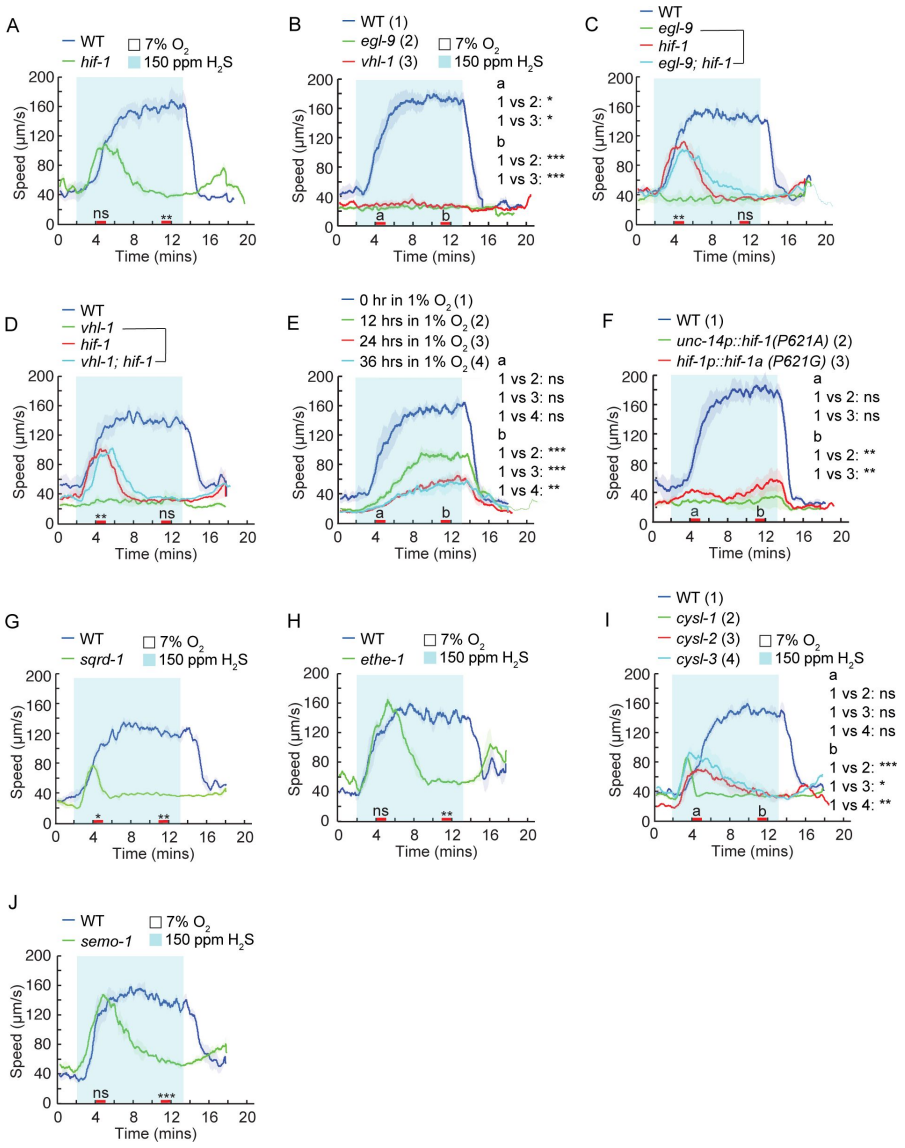

Figure 4.

Acute response to H_2S is modulated by HIF-1 signaling

(**A–D**) Locomotory responses to a switch from 7% O_2 to 150 ppm H_2S balanced with 7% O_2 for animals of the indicated genotype: WT and *hif-1(ia4)* (**A**); WT, *egl-9(sa307) and vhl-1(ok161)* (**B**); WT, *egl-9(sa307), hif-1(ia4) and egl-9(sa307); hif-1(ia4)* double mutants (**C**); WT, *vhl-1(ok161), hif-1(ia4) and vhl-1(ok161); hif-1(ia4)* double mutants (**D**). Red bars on the x-axis represent two intervals (4–5 minutes and 11–12 minutes, labeled as a and b respectively), used for statistical analyses. *** = $p < 0.001$, ** = $p < 0.01$, * = $p < 0.05$, ns = not significant, Mann–Whitney U test. (**E**) Locomotory responses of WT animals to a switch from 7% O_2 to 150 ppm H_2S balanced with 7% O_2 after 0, 12, 24 or 36 hours in 1% O_2. Red bars on the x-axis represent two intervals (4–5 minutes and 11–12 minutes, labeled as a and b respectively), used for statistical analyses. *** = $p < 0.001$, ** = $p < 0.01$, ns = not significant, Mann–Whitney U test. (**F**) Locomotory responses to a switch from 7% O_2 to 150 ppm H_2S balanced with 7% O_2 for animals carrying the non-degradable form of HIF-1. Non-degradable form of HIF-1 (P621A and P621G) are expressed from a pan-neuronal promoter *unc-14* or form *hif-1* endogenous promoter, respectively. Red bars on the x-axis represent two intervals (4–5 minutes and 11–12 minutes, labeled as a and b respectively), used for statistical analyses. ** = $p < 0.01$, ns = not significant, Mann–Whitney U test. (**G–J**) Locomotory responses to a switch from 7% O_2 to 150 ppm H_2S balanced with 7% O_2 for animals of the indicated genotype: WT and *sqrd-1(tm3378)* (**G**); WT and *ethe-1(yum2895)* (**H**); WT, *cysl-1(ok762), cysl-2(ok3516)* and *cysl-3(yum4)* (**I**); WT and *semo-1(yum2889)* (**J**). Red bars on the x-axis represent two intervals (4–5 minutes and 11–12 minutes, labeled as a and b respectively), used for statistical analyses. *** = $p < 0.001$, ** = $p < 0.01$, * = $p < 0.05$, ns = not significant, Mann–Whitney U test.

responses to H_2S. It has been reported that hypoxia inhibits the expression of *ftn-1* and *ftn-2*, while upregulating *smf-3* expression (Ackerman & Gems, 2012; Gourley et al., 2003; Romney et al., 2011). Additionally, *hif-1* mutants have been reported to display reduced intracellular iron content and increased susceptibility to iron starvation (Rajan et al., 2019; Romney et al., 2011). We explored if the locomotory defect of *hif-1* mutants in H_2S could be explained by iron deficiency (Rajan et al., 2019; Romney et al., 2011). The presence of FAC significantly improved H_2S evoked locomotory activity of *hif-1* mutants (***Figure 5F***). In addition, disrupting *ftn-1* partially suppressed the locomotory defect of *hif-1* mutants in H_2S (***Figure 5G***). These data confirm that labile iron pool is critical to maintain the locomotory activity of animals in H_2S.

Iron deficiency causes mitochondrial dysfunction including decreased cytochrome concentration and respiratory efficiency (Dallman, 1986; Masini, Salvioli, et al., 1994; Masini, Trenti, et al., 1994; Walter et al., 2002). H_2S is known to exert both positive and negative effects on the mitochondria, which are not only the primary targets of H_2S but also represent one of the main cellular hubs of H_2S detoxification (Cooper & Brown, 2008; Khan et al., 1990; Nicholls & Kim, 1982a). We probed the possibility that impairing mitochondrial function might alter locomotory response to H_2S. To this end, we tested mutants with the disruption of *gas-1*, *clk-1*, *mev-1*, or *isp-1* genes. Similar to iron depletion, these mutants abrogated locomotory response to H_2S (***Figure 6A–D***). Additionally, exposing animals to the mitochondrial complex I inhibitor rotenone fully repressed locomotory response to H_2S (***Figure 6E***). While rotenone exposure inhibits H_2S response, it evoked increased locomotory activity over 2 hours (***Figure 6E***). These observations confirm the critical role of mitochondria in supporting locomotory response in exposure to H_2S in *C. elegans*.

Discussion

Animals' behavior and physiology are profoundly influenced by the surrounding environment, in which they reside. Wild *C. elegans* isolates thrive in the decomposing matters, where the local concentrations of O_2 are low while the levels of CO_2 and H_2S could be high. These animals have adapted their behavior in such an environment, displaying increased sensitivity to high O_2 exposure but dampened responses to CO_2. In contrast, the standard laboratory strain N2, which is constantly exposed to high O_2 but low CO_2, is relatively insensitive to elevated levels of O_2 but robustly avoids CO_2 exposure (Beets et al., 2020; Bretscher et al., 2008; Carrillo et al., 2013; Hallem & Sternberg, 2008). As observed in response to CO_2, N2 animals exhibit strong reorientation and acceleration to escape the H_2S exposure, while wild isolates display a significantly diminished response to H_2S.

The responses to CO_2 and H_2S in N2 animals are modulated by common signaling pathways, which include the ciliogenesis, the cGMP-gated channels TAX-2 and TAX-4, calcineurin subunit TAX-6/CNB-1, and nuclear hormone receptor NHR-49. Additionally, these two responses are affected by the nutritional state of the animals. In *C. elegans*, starvation is signaled by reduced activity in two major signaling pathways: the insulin and TGF-β pathways. H_2S and CO_2 responses are abolished in starved animals or mutants that disrupt insulin or TGF-β signaling. Therefore, the modulation of behavioral responses to H_2S and CO_2 by external and internal factors appears highly similar. However, CO_2 response is mediated by the guanylate cyclase GCY-9 in BAG neurons (Hallem et al., 2011), which appears to be dispensable for H_2S sensing. We observed a prominent role for the guanylate cyclase DAF-11 expressed in the chemosensory neurons ASJ for H_2S responses. *daf-11* signaling in ASJ also mediates chemosensory responses to volatile chemicals and to NO (Birnby et al., 2000; Hao et al., 2018). However, DAF-11 controls the normal larval development of *C. elegans* and may have pleiotropic indirect effects on sensory functions (Murakami, Koga, & Ohshima, 2001). In absence of more direct evidence, its role as H_2S sensor in ASJ remain uncertain.

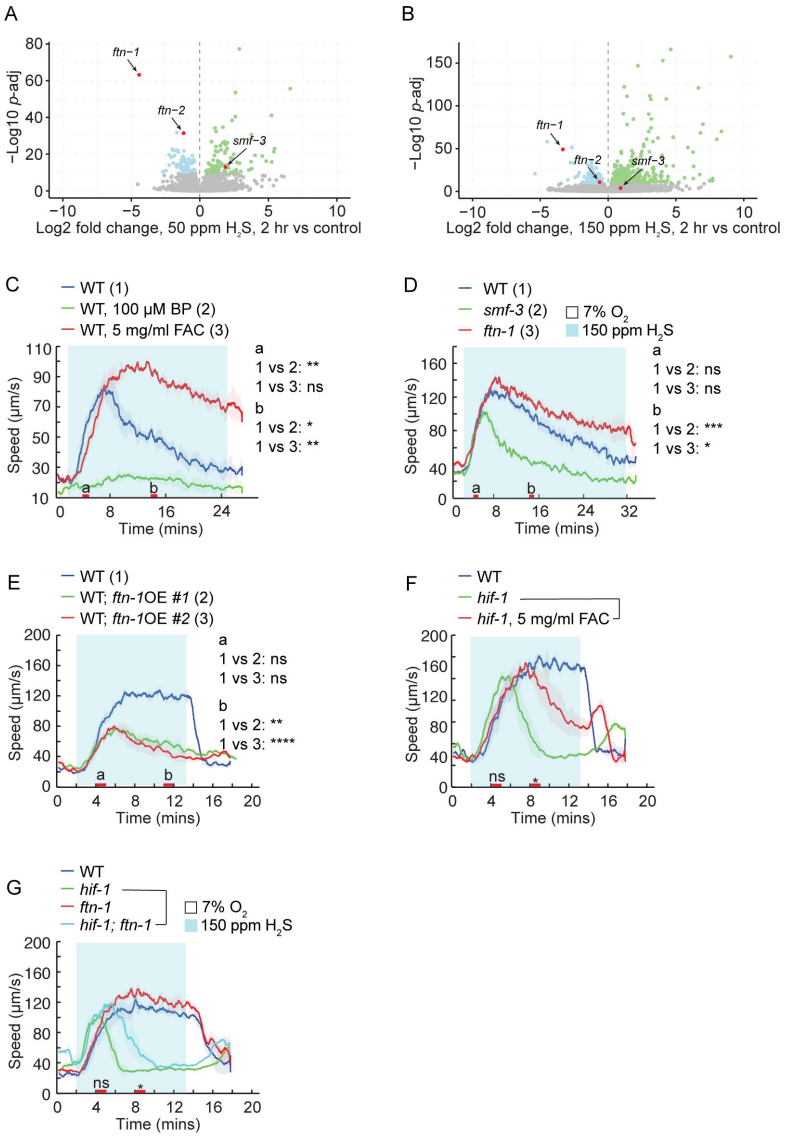

Figure 5.

Labile iron pool is critical to sustain the locomotory activity in H_2S

(**A, B**) Volcano plots showing the relative expression of the genes involved in the regulation of iron homeostasis in WT animals after 2-hour exposure with 50 ppm (**A**) or 150 ppm (**B**) H_2S balanced with 7% O_2. (**C**) Locomotory responses to a switch from 7% O_2 to 150 ppm H_2S balanced with 7% O_2 for WT animals, WT animals pretreated with 100 μM 2,2'-Bipyridyl (BP) and WT animals pretreated with 5 mg/ml ferric ammonium citrate (FAC) in the presence of food for 16 hours. Red bars on the x-axis represent two intervals (4–5 minutes and 14–15 minutes, labeled as a and b respectively), used for statistical analyses. ** = $p < 0.01$, * = $p < 0.05$, ns = not significant, Mann–Whitney U test. (**D**) Locomotory responses to a switch from 7% O_2 to 150 ppm H_2S balanced with 7% O_2 for animals of the indicated genotype: WT, *smf-3(ok1305)* and *ftn-1(ok3625).* Red bars on the x-axis represent two intervals (4–5 minutes and 14–15 minutes, labeled as a and b respectively), used for statistical analysis. *** = $p < 0.001$, * = $p < 0.05$, ns = not significant, Mann–Whitney U test. (**E**) Locomotory responses to a switch from 7% O_2 to 150 ppm H_2S balanced with 7% O_2 for WT animals and animals overexpressing *ftn-1* genomic DNA under its own promoter (#1 and #2 indicate two independent lines). Red bars on the x-axis represent two intervals (4–5 minutes and 11–12 minutes, labeled as a and b respectively), used for statistical analysis. **** = $p < 0.0001$, ** = $p < 0.01$, ns = not significant, Mann–Whitney U test. (**F, G**) Locomotory responses to a switch from 7% O_2 to 150 ppm H_2S balanced with 7% O_2 for animals of the indicated genotype: WT, *hif-1(ia4)* and *hif-1(ia4)* mutants pretreated with 5 mg/ml ferric ammonium citrate (FAC) for 16 hours (**F**); WT, *hif-1(ia4), ftn-1(ok3625)* and *hif-1(ia4); ftn-1(ok3625)* double mutants (**G**). Red bars on the x-axis represent two intervals (4–5 minutes and 8–9 minutes) used for statistical analysis. * = $p < 0.05$, ns = not significant, Mann– Whitney U test.

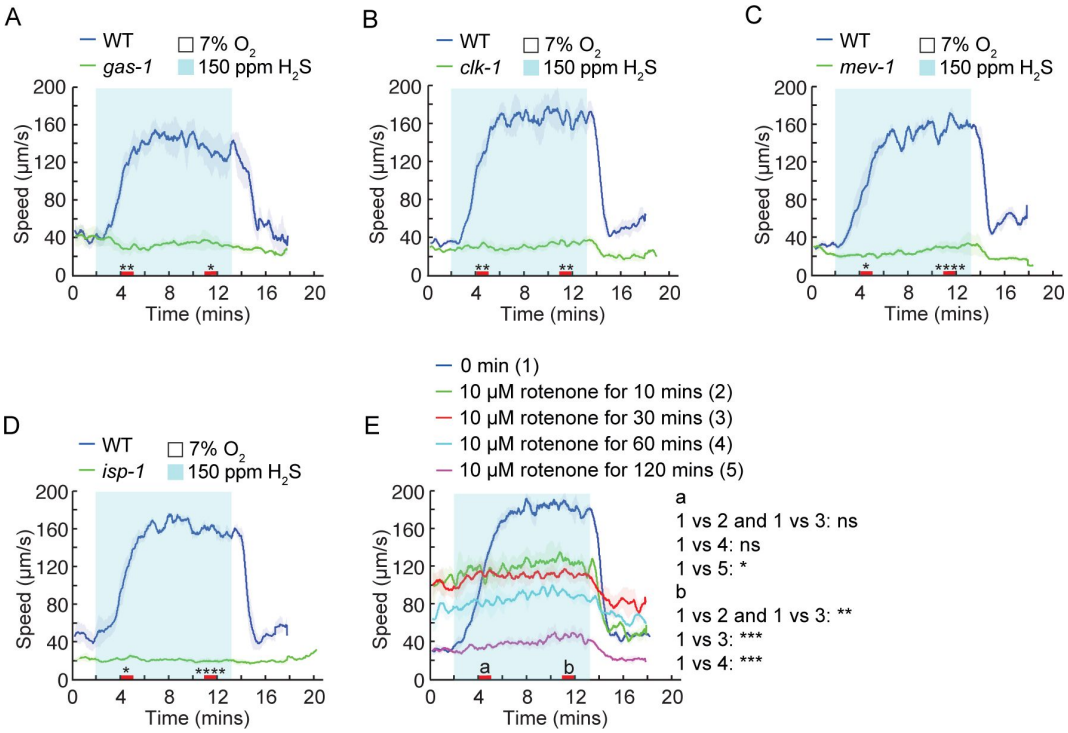

Figure 6.

Mitochondrial function is required for acute response to H_2S

(**A–D**) Locomotory responses to a switch from 7% O_2 to 150 ppm H_2S balanced with 7% O_2 for animals of the indicated genotype: WT and *gas-1(fc21)* (**A**); WT and *clk-1(qm30)* (**B**); WT and *mev-1(kn1)* (**C**); WT and *isp-1(qm150)* (**D**). Red bars on the x-axis represent two intervals (4–5 minutes and 11–12 minutes) used for statistical analysis. **** = $p < 0.0001$, ** = $p < 0.01$, * = $p < 0.05$, Mann–Whitney U test. (**E**) Locomotory responses to a switch from 7% O_2 to 150 ppm H_2S balanced with 7% O_2 for WT animals pretreated with 10 µM rotenone for 0 minute, 10 minutes, 30 minutes, 60 minutes or 120 minutes. Red bars on the x-axis represent two intervals (4–5 minutes and 11–12 minutes, labeled as a and b respectively), used for statistical analysis. *** = $p < 0.001$, ** = $p < 0.01$, * = $p < 0.05$, ns = not significant, Mann–Whitney U test.

Long-term exposure to H_2S can elicit adaptive responses including changes in gene expression patterns to mitigate the toxic effects of H_2S. Within just one hour of H_2S exposure, we observed the upregulation of genes associated with H_2S detoxification. This response enables animals to detoxify H_2S and maintain cellular homeostasis under sulfidic conditions. This adaptive strategy is accompanied by the reduced locomotory response to H_2S exposure. The HIF-1 (hypoxia-inducible factor) signaling is a major pathway involved in the adaption during prolonged H_2S exposure (Budde & Roth, 2011; Miller et al., 2011b). When the HIF-1 pathway is constitutively induced in the nervous system, the behavioral responses to H_2S are eliminated. Similarly, reduced behavioral responses to H_2S are observed after 12 hours of exposure to 1% O_2. It has been proposed that persulfides, polysulfides, and thiosulfate, which are the by-products during sulfide detoxification, play a role in H_2S signaling (Mishanina, Libiad, & Banerjee, 2015). However, in the case of locomotion responses to H_2S in *C. elegans*, this is unlikely to be the mechanism for the initial response, as mutants lacking detoxification enzymes still exhibit an acute and transient response to H_2S. Interestingly, the sustained locomotory activity was abolished in these mutants, suggesting that either the by-products of H_2S detoxification contribute to maintain the behavioral response or the lack of detoxification enzyme results in rapid cellular toxicity, preventing sustained locomotory activity in H_2S (Budde & Roth, 2011).

Interestingly, we provide evidence that labile iron pool is critical for H_2S responses. Removal of labile iron pool by the chelator BP or *ftn-1* overexpression attenuated both acute and sustained responses to H_2S, suggesting that intracellular iron is required for the sensation of H_2S. While increasing labile iron levels sustains the locomotory activity in H_2S. In *C. elegans*, labile iron homeostasis is predominantly regulated by the HIF-1 signaling, the activation of which decreases the transcription of *ftn-1* and increases the expression of *smf-3* (Ackerman & Gems, 2012; Romney et al., 2011). Consistent with this, we have observed a downregulation of the ferritins FTN-1 and FTN-2, as well as an upregulation of the iron transporter SMF-3 during exposure to H_2S. This suggests that H_2S may control the expression of FTN-1 and SMF-3, and consequently the labile iron pool, through the HIF-1 pathway.

Although the exact mechanisms are not yet fully understood, several possibilities shed light on the importance of labile iron for H_2S responses. Fe^{2+} acts as a critical cofactor for the PHD/EGL-9 enzymes, which are involved in the hydroxylation-dependent destabilization of HIF-1 (Myllyharju & Kivirikko, 1997). PHD inactivation by iron sequestration by ferritin can increase HIF-1 signaling, suggesting a potential role of labile iron as a negative feedback loop to limit HIF-1 activity (Siegert et al., 2015). In addition, iron is necessary for the biosynthesis of iron-sulfur (Fe-S) clusters, critical cofactors involved in redox reactions and mitochondrial respiration (Read, Bentley, Archer, & Dunham-Snary, 2021; Xu & Moller, 2011). Labile iron is beneficial for the biogenesis of Fe-S clusters despite its oxidative properties under normal O_2 conditions (Liochev, 1996). Interestingly, hypoxia has been observed to enhance Fe-S cluster biogenesis by increasing the availability of bioactive iron (Ast et al., 2019). Therefore, low oxidative stress may alleviate the need to maintain a low labile iron pool. In this context, the antioxidant properties of H_2S or the interruption of mitochondrial respiration by H_2S might provide condition favorable to high labile iron pool (Shefa, Kim, Jeong, & Jung, 2018; Sunda, Kieber, Kiene, & Huntsman, 2002).

The primary mechanism underlying the toxic effects of H_2S has been suggested to be the direct inhibition of cytochrome c oxidase, a critical enzyme involved in mitochondrial respiration (Cooper & Brown, 2008; Khan et al., 1990; Nicholls & Kim, 1982b). Intriguingly, we have observed that genetic and pharmacological inhibition of mitochondrial respiration prevents the locomotory response of *C. elegans* to H_2S. This effect may be mediated by the induction of the HIF-1 pathway, which has been observed in mutants with impaired mitochondrial respiration (Lee, Hwang, & Kenyon, 2010). Furthermore, acute inhibition of mitochondrial respiration by rotenone also enhances locomotion while suppressing the response to H_2S. Reducing mitochondrial respiration has been found to stimulate aversive behavior in *C. elegans* (Melo &

Ruvkun, 2012). Therefore, the acute inhibition of mitochondrial respiration by H_2S could transiently promote aversive behavior in *C. elegans*, while long-term inhibition of mitochondrial respiration may contribute to the induction of the HIF-1 pathway and adaptation to H_2S.

In summary, this study unveils a novel behavior of *C. elegans* in their avoidance to H_2S. The response to H_2S is intricately shaped by their environment, where it integrates with other sensory signals, including food availability, CO_2 and O_2 levels. We emphasize the vital role of H_2S detoxification system, particularly the involvement of mitochondria and labile irons, in sustaining the locomotory activity in H_2S. In the future, it will be exciting to elucidate the neuronal mechanisms driving H_2S avoidance and to explore how the changes of labile iron pools modulate cellular and organismal behavior responses to noxious sensory stimuli.

Materials and Methods

Strains

C. elegans were maintained using standard protocols (Brenner, 1974). Strains used in this study are listed in ***Supplementary file 1*** and ***Supplementary file 3***.

Preparation of H_2S gas mixture

Different H_2S concentrations were created as previously described (Miller & Roth, 2007). Briefly, the H_2S-containing gas mixture were prepared by diluting 5000 ppm H_2S in nitrogen (N_2) with 7% O_2 balanced with N_2. The gas flow was tuned by Sierra Smart-Trak 100 mass flow controllers. H_2S concentration in the mixture was measured using two H_2S detectors (MSA ALTAIR 2X gas detector for H_2S and Clip Single Gas Detector, SDG, CROWCON). The pre-defined gas mixtures of 7% O_2, 1% O_2 and 5% CO_2 with N_2 were purchased from Air Liquide Gas AB. 5000 ppm H_2S stock in N_2 was obtained from Linde Gas AB. Gas mixtures in all experiments were hydrated before use.

Molecular Biology

The Multisite Gateway system (Thermo Fisher Scientific, United States) was used to generate expression vectors. Promoters, including *gcy-37* (2.7kb), *trx-1* (1 kb), *ftn-1*(2 kb), *daf-11*(3 kb), *odr-3*(2.7 kb), *gpa-11*(3 kb), *sra-6*(3 kb), *odr-1*(2.4 kb), *flp-21*(4.1kb), and *ocr-2*(2.4 kb) were amplified from N2 genomic DNA and cloned into pDONR P4P1 using BP clonase. *gcy-35*, *tax-4* and *pkc-1* cDNAs were amplified using the first strand cDNA library as the template, while *daf-11* and *ftn-1* genomic sequences were amplified using genomic DNA as the template. The entry clones of these genes pDONR 221 were generated using BP reaction. To generate the gain of function mutation of *pkc-1* (A160E), Q5 Site-Directed Mutagenesis Kit (NEB) was used according to manufacturer instructions. All expression vectors were generated using LR reaction. The primer sequences were displayed in ***Supplementary file 4***.

To generate transgenic animals, the *daf-11* expression vectors were injected at the concentration of 20 ng/µl supplemented with 50 ng/µl of a coelomocyte co-injection marker (*unc-122p::GFP)* and 30 ng/µl of 1kb DNA ladder. For *tax-4* gene, the injection mixtures were prepared using 40 ng/µl of *tax-4* expression vectors, 50 ng/µl of a coelomocyte co-injection marker and 10 ng/µl of 1kb DNA ladder. The rest of expression constructs were injected at 50 ng/µl together with 50 ng/µl of a coelomocyte marker.

CRISPR/Cas9 genome editing

Genes were disrupted using CRISPR/Cas-9 mediated genome editing as described (Dokshin, Ghanta, Piscopo, & Mello, 2018; Ghanta & Mello, 2020). The strategy involved the utilization of homology-directed insertion of custom designed single strand DNA template (ssODN), which had

two homology arms of 35bp flanking the targeted PAM site. Between two homology arms, a short sequence containing a unique restriction enzyme cutting site and in frame as well as out of frame stop codons was included. The insertion of ssODN template would delete 16 bases of coding sequence, ensuring the proper gene disruption. To prepare the injection cocktail, 0.5 µl of Cas-9 protein (IDT) was mixed with 5 µl of 0.4µg/µl tracrRNA (IDT, United States) and 2.8 µl of 0.4 µg/µl crRNA (IDT). The mixture was incubated at 37°C for at least 10 minutes before 2.2 µl of 1µg/µl ssODN (or 500 ng dsDNA) and 2 µl of 0.6 µg/µl *rol-6* co-injection marker were added. Nuclease-free water was used to bring the final volume to 20 µl. The injection mixture was centrifuged for 2 minutes before use.

Behavioral assays

H_2S evoked locomotion activity was monitored as described previously (Laurent et al., 2015; Zhao et al., 2022). Briefly, OP50 bacteria were seeded on the assay plates 16 hours before use. The border of bacterial lawn was removed using a PDMS stamp. For each assay, 25 to 30 day-one adult animals were picked onto assay plates, allowed to settle down for 15 minutes, and subsequently sealed within microfluidic chambers. A syringe pump (PHD 2000, Harvard Apparatus) was employed to deliver gas mixtures into the microfluidic chamber at a constant flow of 3 ml/min. The rapid switch between different gas mixtures were controlled by Telfon valves coupled with ValveBank Perfusion Controller (AutoMate Scientific). The locomotory activity at different gas mixtures were monitored using a high-resolution camera (FLIR) mounted on a Zeiss Stemi 508 microscope. Videos were captured at a rate of 2 frames per second, starting with a 2-minute recording in 7% O_2, followed by 11 minutes in H_2S, and ending with a final 5-minute period in 7% O_2. For the long-term recording in H_2S, video capture commenced with a 2-minute period in 7% O_2, followed by a duration of 148 minutes in 150 ppm H_2S, and concluded with a final 2-minute interval in 7% O_2.

To assess the effects of rotenone on H_2S evoked locomotory response, day-one adult animals were subjected to 10 µM rotenone for 10min, 30min, 1 hour and 2 hours on the drug containing plates. Subsequently, the rotenone-treated animals were assayed on the standard assay plates without the drug. To explore the impact of ferric ammonium citrate (FAC) (F5879, Sigma-Aldrich) and 2,2'-Bipyridyl (BP) (D216305, Sigma-Aldrich) on behavioral response to H_2S, L4 animals were exposed to 100 µM FAC or 5mg/ml BP for 16 hours in the presence of bacterial food. The FAC or BP treated animals were assayed on FAC or BP containing plates.

Optogenetic experiments were performed as previously outlined (Zhao et al., 2022). Transgenic L4 animals were exposed to 100µM all-trans retinal (ATR) (R2500, Sigma) in the dark for 16 hours. The ATR-fed animals were assayed with the illumination of 70 µW/mm^2 blue light during the whole assay period. Blue light was emitted from an ultra-high-power LED lamp (UHP-MIC-LED-460, Prizmatix), and the light intensity was determined using a PM50 Optical Power Meter (ThorLabs). To minimize the effect of transmitted light on the transgenic animals, a long-pass optical filter was used to eliminate the lights with short wavelengths during picking. All videos of behavioral analysis were analyzed using a home-made MATLAB program Zentracker (*https://github.com/wormtracker/zentracker*). For all behavior analyses, at least three assays were performed for each strain with more than 80 worms in total.

RNA extraction and sequencing

To obtain RNA samples for RNA-seq, thirty young adult animals were picked to each fresh plate and allowed to lay eggs for 2 hours, after which the adult animals were removed and eggs were allowed to develop into day one adults. Day one animals were subsequently challenged with H_2S for three different time points (1 hour, 2 hours and 12 hours). For each time point, five plates of day one animals were exposed to 50 ppm H_2S, 150 ppm H_2S or 7% O_2 as a control group. Subsequently, the animals were immediately collected and rinsed three times with M9 buffer. After washing, the worm pellet was frozen in liquid nitrogen. Animals were homogenized using

Bullet Blender (Next Advance) in the presence of Qiazol Lysis Reagent and 0.5mm Zirconia beads at 4°C. RNA was prepared using RNeasy Plus Universal Mini Kit (Qiagen). Six independent RNA samples were prepared for all different treatments. The 2100 Bioanalyzer instrument (Agilent) was used for the RNA quality control with a microfluidic chip specific for RNA (Agilent RNA 6000 Nano Kit). Then 1 µg of qualified RNA samples in RNase-free ddH2O was used for library preparation. Library was constructed and sequenced by Novogene.

RNA-seq analysis

The RNA-seq data was aligned using STAR v2.7.9a (Dobin et al., 2013) and gene expression counts extracted by featureCounts v2.0.3 (Liao, Smyth, & Shi, 2014). Differential expression was calculated using DESeq2 (Love, Huber, & Anders, 2014). GO analysis was performed using the EnrichR R package (Kuleshov et al., 2016) on genes having *p*.adj < 1e-10. For brevity, several highly similar GO categories were manually omitted (full EnrichR output available at Github repository).

Data availability

Raw sequencing data has been deposited at ArrayExpress # E-MTAB-13296. The R code is available at *https://github.com/henriksson-lab/ce_h2s_tc*.

Acknowledgements

We thank the Caenorhabditis Genetics Center (funded by NIH Office of Research Infrastructure Programs P40 OD010440) and the National BioResources Project Japan for strains.

Funding

The computations were enabled by resources provided by the National Academic Infrastructure for Supercomputing in Sweden (NAISS) and the Swedish National Infrastructure for Computing (SNIC) at UPPMAX partially funded by the Swedish Research Council through grant agreements no. 2022-06725 and no. 2018-05973. This work is supported by the Swedish VR Research Council grant MIMS (2021-06602) to J.H., the Belgian National Fund for Scientific Research (FRS-FNRS) to P.L., the ERC starting grant (802653 OXYGEN SENSING), the Swedish Research Council VR starting grant (2018-02216), and the Wallenberg Centre for Molecular Medicine (Umeå) to C.C.

Figure legends

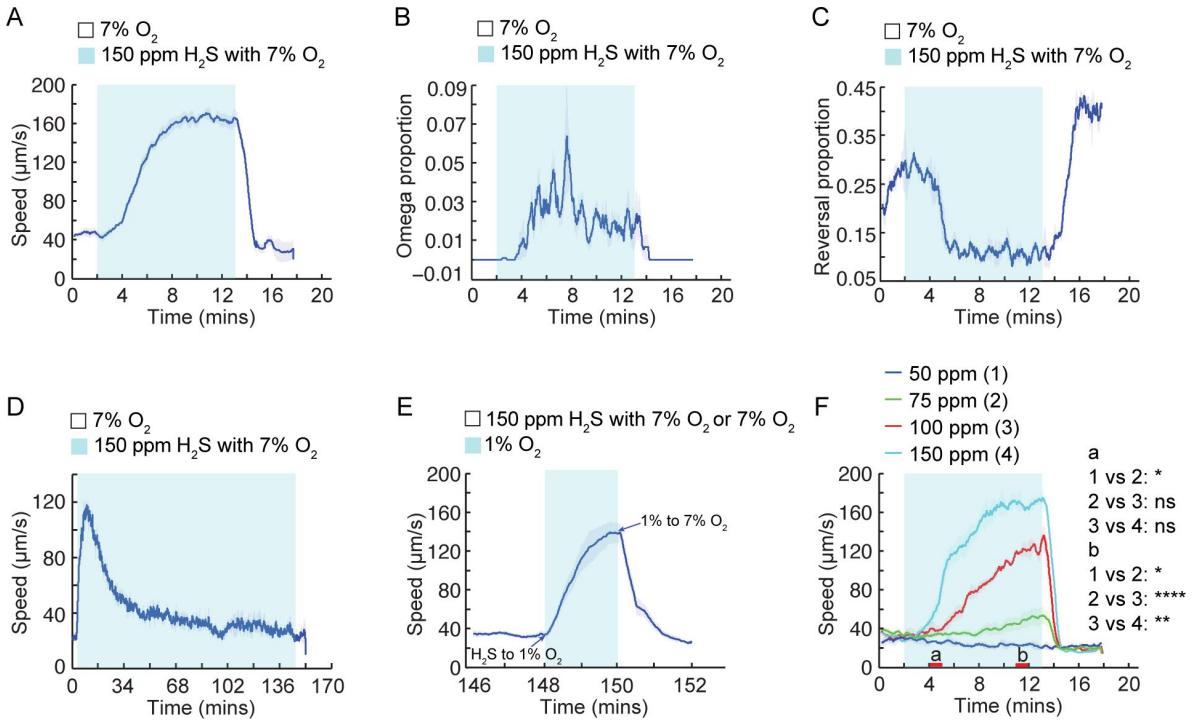

Figure 1—figure supplement 1.

Acute locomotory responses of *C. elegans* to hydrogen sulfide.

(**A**) Changes in the locomotory activity of WT animals evoked by a switch from 7% O_2 to 150 ppm H_2S balanced with 7% O_2. (**B**) Reorientation movements (omega turns) of WT animals evoked by a switch from 7% O_2 to 150 ppm H_2S balanced with 7% O_2. (**C**) Changes in reversal frequency in WT animals experiencing a switch from 7% O_2 to 150 ppm H_2S balanced with 7% O_2. (**D**) Locomotory activity of WT was recorded for 2 minutes at 7% O_2 and 148 minutes at 150 ppm H_2S balanced with 7% O_2 followed by 2 additional minutes at 7% O_2. (**E**) Locomotory activity of WT animals evoked by acute hypoxia after preincubation for 148 minutes at 150 ppm H_2S balanced with 7% O_2. Locomotory activity was recorded for 2 minutes at each gas interval. (**F**) Locomotory responses of WT animals to different concentrations of H_2S balanced with 7% O_2. Red bars on the x-axis represent two intervals (4–5 minutes and 11–12 minutes, labeled as a and b respectively) used for statistical analysis. **** = $p < 0.0001$, ** = $p < 0.01$, * = $p < 0.05$, ns = not significant, Mann–Whitney U test.

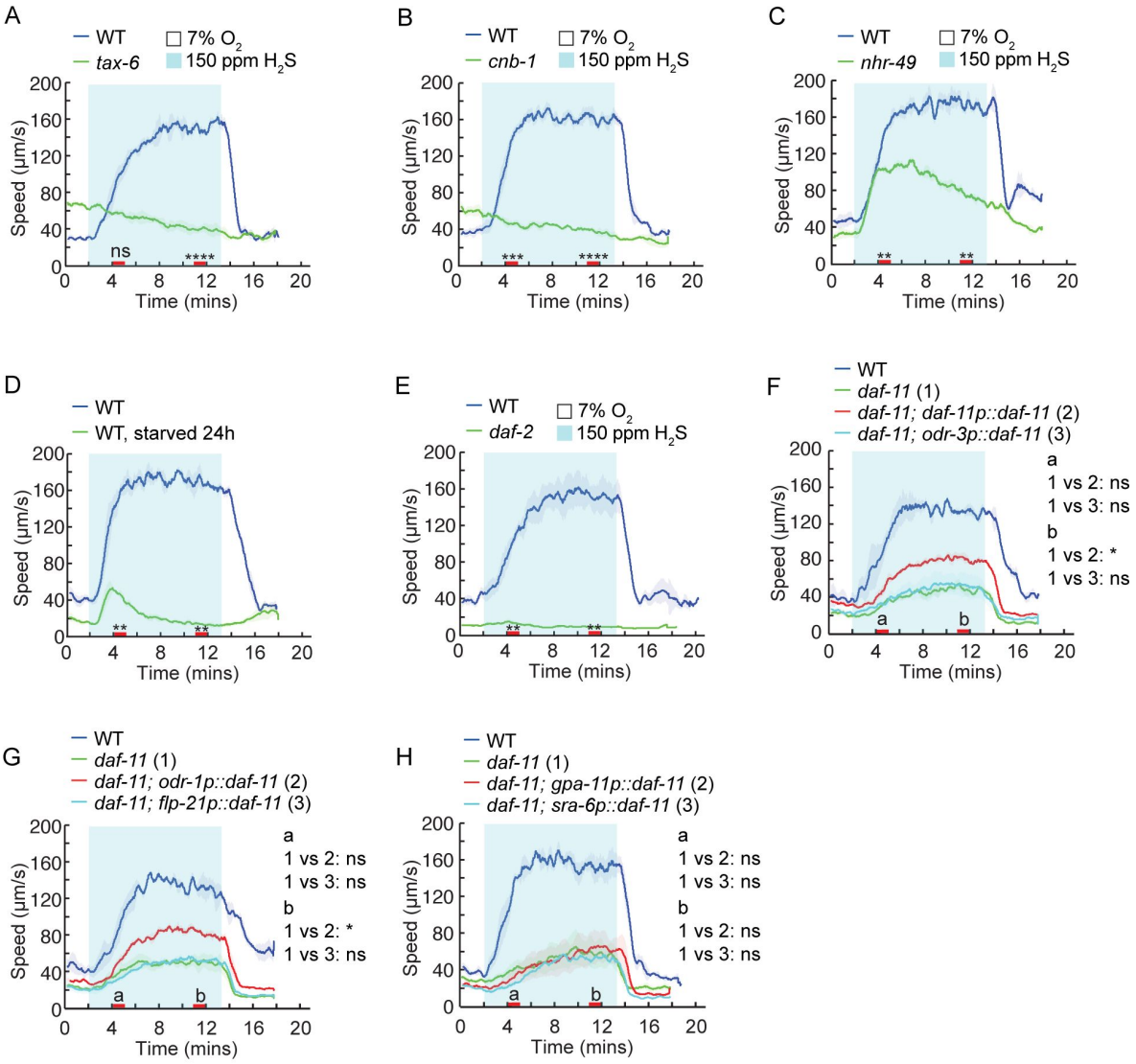

I

Promoter	neurons														
Pdaf-11	ASH	AWB	AWC	ASJ	ASK	ADL	ASI	ASE							
Podr-3	ASH	AWB	AWC						ADF	AWA					
Podr-1		AWB	AWC	ASJ	ASK		ASI								
Pflp-21	ASH					ADL	ASI	ASE			FLP	URA	RMG	MC	M2	M4
Pgpa-11	ASH					ADL									
Psra-6	ASH						ASI								PVQ

Figure 1—figure supplement 2.

Acute response to H_2S is regulated by multiple signaling pathways

(**A–E**) Locomotory responses to a switch from 7% O_2 to 150 ppm H_2S balanced with 7% O_2 for animals of the indicated genotype: WT and *tax-6(ok2065)* (**A**); WT and *cnb-1(ok276)* (**B**); WT and *nhr-49(nr2041)* (**C**); WT animals and WT animals starved for 24 hours (**D**); WT and *daf-2(e1370)* (**E**). To assay *daf-2* animals, WT and *daf-2* mutants were kept in 15°C. L4 animals were picked, maintained at 25°C until day-one adults and assayed at room temperature. Red bars on the x-axis represent two intervals (4–5 minutes and 11–12 minutes), used for statistical analysis. **** = $p < 0.0001$, *** = $p < 0.001$, ** = $p < 0.01$, ns = not significant, Mann–Whitney U test. (**F–I**) Locomotory responses to a switch from 7% O_2 to 150 ppm H_2S balanced with 7% O_2 for animals of the indicated genotype: WT, *daf-11(m47)* and transgenic *daf-11* mutants expressing *daf-11* genomic DNA in different subsets of neurons (**F–H**); The detailed expression pattern of each promoter is listed in (**I**). Red bars on the x-axis represent two intervals (4–5 minutes and 11–12 minutes, labeled as a and b respectively), used for statistical analysis. * = $p <$ 0.05, ns = not significant, Mann–Whitney U test.

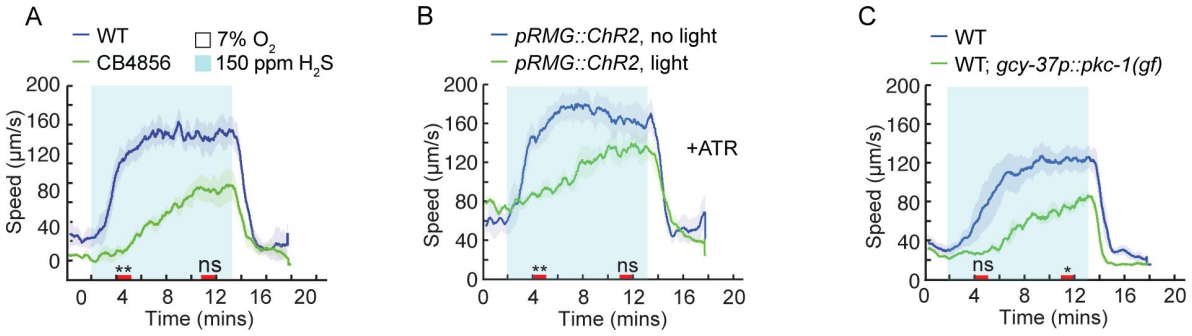

Figure 2—figure supplement 1.

NPR-1 signaling modulates locomotory response to H_2S

(**A**) Locomotory responses to a switch from 7% O_2 to 150 ppm H_2S balanced with 7% O_2 for WT animals and wild isolate CB4856. Red bars on the x-axis represent two intervals (4–5 minutes and 11–12 minutes), used for statistical analysis. ** = $p < 0.01$, ns = not significant, Mann–Whitney U test. (**B**) Optogenetic stimulation of RMG neurons using channelrhodopsin-2 (ChR2). Expressing ChR2 in RMG neurons were achieved using Cre-LoxP system (Macosko et al., 2009). L4 animals were picked, grown for 16 hours on the seeded plates containing ATR, and assayed as day-one adults. Blue light was delivered throughout the assay. Red bars on the x-axis represent two intervals (4–5 minutes and 11–12 minutes), used for statistical analysis. ** = $p < 0.01$, ns = not significant, Mann–Whitney U test. (**C**) Activation of O_2 sensing neurons by expressing a gain-of-function allele of *pkc-1* under *gcy-37* promoter. Red bars on the x-axis represent two intervals (4–5 minutes and 11– 12 minutes), used for statistical analysis. * = $p < 0.05$, ns = not significant, Mann–Whitney U test.

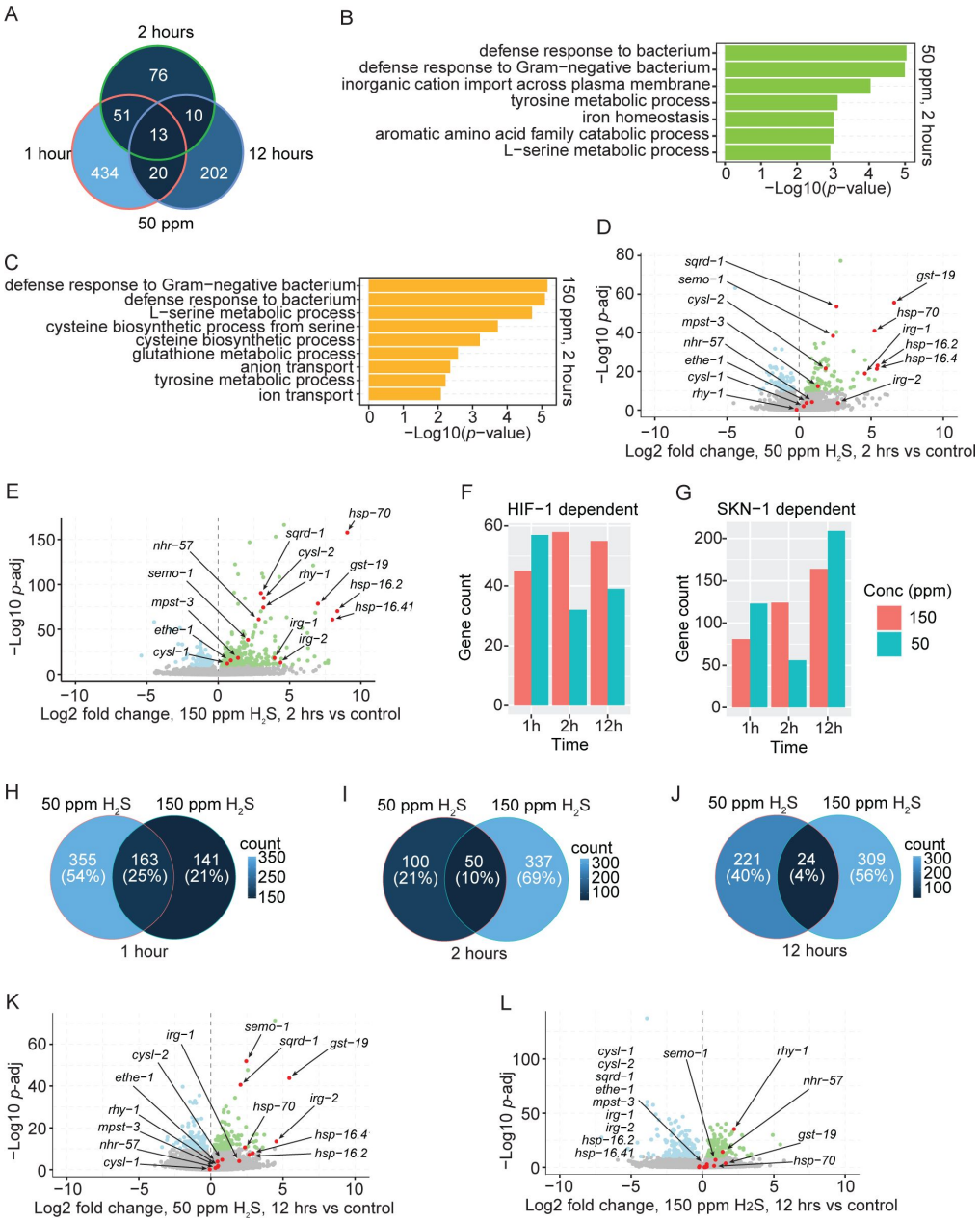

Figure 3—figure supplement 1.

Transcriptome reprogramming induced by H_2S exposure

(**A**) Venn diagram displaying the number of differentially expressed genes after exposure in 50 ppm H_2S balanced with 7% O_2 in WT animals for 1 hour, 2 hours or 12 hours. Adjusted *p* value <1e-10. (**B, C**) Significantly enriched GO categories for differentially expressed genes with adjusted *p* value <1e-10 in WT animals exposed to 50 ppm (**B**) or 150 ppm (**C**) H_2S balanced with 7% O_2 for 2 hours. (**D, E**) Volcano plot showing the differentially expressed genes with adjusted *p* value <1e-10 in WT animals exposed to 50 ppm (**D**) or 150 ppm (**E**) H_2S balanced with 7% O_2 for 2 hours. A set of genes involved in H_2S detoxification, cysteine metabolism and stress response were highlighted in red. (**F, G**) The number of HIF-1(**F**) and SKN-1(**G**) target genes induced by 50 ppm or 150 ppm H_2S exposure for 1hour, 2 hours or 12 hours in WT animals, with Adjusted *p* value < 1e-30. (**H–J**) Venn diagrams displaying the number of differentially expressed genes (adjusted *p* value <1e-10) in WT animals of the indicated conditions: animals were exposed to 50 ppm or 150 ppm H_2S for 1hour (**H**); for 2hours (**I**); and for 12 hours (**J**). (**K, L**) Volcano plots showing the differentially expressed genes (adjusted *p* value <1e-10) in WT animals that were exposed to either 50 ppm (**K**) or 150 ppm (**L**) H_2S balanced with 7% O_2 for 12 hours. A set of genes involved in H_2S detoxification, cysteine metabolism and stress response were highlighted in red.

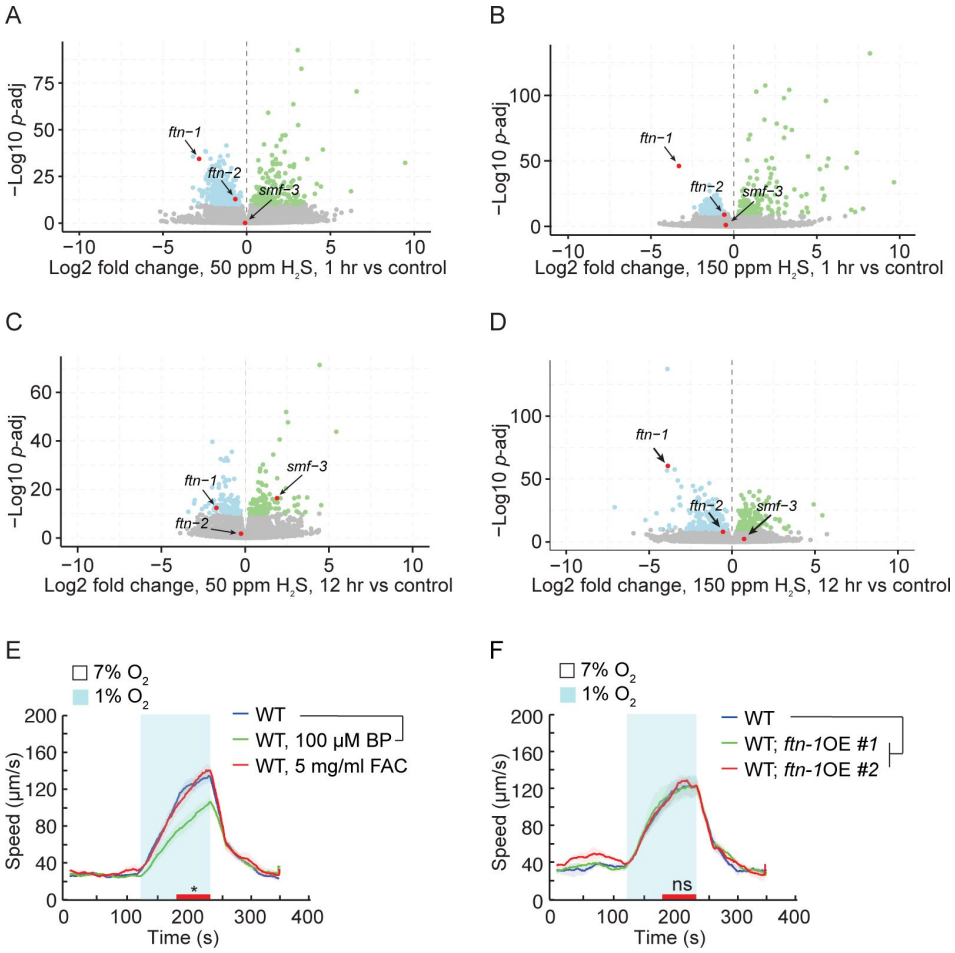

Figure 5—figure supplement 1.

ftn-1 expression is consistently repressed in H_2S

(**A–D**) Volcano plots showing the relative expression of the genes involved in the regulation of iron homeostasis (*ftn-1*, *ftn-2* and *smf-3*) in WT animals of the indicated conditions: 1-hour exposure in 50 ppm H_2S balanced with 7% O_2 (**A**); 1-hour exposure in 150 ppm H_2S balanced with 7% O_2 (**B**); 12-hour exposure in 50 ppm H_2S balanced with 7% O_2 (**C**); and 12-hour exposure in 150 ppm H_2S balanced with 7% O_2 (**D**). (**E, F**) Locomotory responses to a switch to 7% to 1% O_2 for animals of the indicated treatments or genotypes: WT animals, WT animals treated with 100 μM 2,2'-Bipyridyl (BP), and WT animals treated with 5 mg/ml ferric ammonium citrate (FAC) for 16 hours (**E**); WT and WT animals overexpressing *ftn-1* genomic DNA under its own promoter (#1 and #2 indicate two independent lines) (**F**). Red bar on the x-axis represents time interval (3–4 minutes) used for statistical analysis. * = $p < 0.05$, ns = not significant, Mann–Whitney U test.

References

Abel D. C., Koenig C. C., Davis W. P. (1987) **Emersion in the Mangrove Forest Fish Rivulus-Marmoratus - a Unique Response to Hydrogen-Sulfide** *Environmental Biology of Fishes* **18**:67–72 https://doi.org/10.1007/Bf00002329

Ackerman D., Gems D. (2012) **Insulin/IGF-1 and Hypoxia Signaling Act in Concert to Regulate Iron Homeostasis in Caenorhabditis elegans** *Plos Genetics* **8** https://doi.org/10.1371/journal.pgen.1002498

Anderson C. P., Leibold E. A. (2014) **Mechanisms of iron metabolism in Caenorhabditis elegans** *Frontiers in Pharmacology* **5** https://doi.org/10.3389/fphar.2014.00113

Ast T., Meisel J. D., Patra S., Wang H., Grange R. M. H., Kim S. H., Mootha V. K. (2019) **Hypoxia Rescues Frataxin Loss by Restoring Iron Sulfur Cluster Biogenesis** *Cell* **177** https://doi.org/10.1016/j.cell.2019.03.045

Beets I., Zhang G., Fenk L. A., Chen C., Nelson G. M., Felix M. A., de Bono M. (2020) **Natural Variation in a Dendritic Scaffold Protein Remodels Experience-Dependent Plasticity by Altering Neuropeptide Expression** *Neuron* **105**:106–121 https://doi.org/10.1016/j.neuron.2019.10.001

Birnby D. A., Link E. M., Vowels J. J., Tian H., Colacurcio P. L., Thomas J. H., Retrieved from <CGO to ISI>://WOS:000086869200008 (2000) **A transmembrane guanylyl cyclase (DAF-11) and Hsp90 (DAF-21) regulate a common set of chemosensory behaviors in Caenorhabditis elegans** *Genetics* **155**:85–104

Brenner S. (1974) **The genetics of Caenorhabditis elegans** *Genetics* **77**:71–94 https://doi.org/10.1093/genetics/77.1.71

Bretscher A. J., Busch K. E., de Bono M. (2008) **A carbon dioxide avoidance behavior is integrated with responses to ambient oxygen and food in Caenorhabditis elegans** *Proc Natl Acad Sci U S A* **105**:8044–8049 https://doi.org/10.1073/pnas.0707607105

Budde M. W., Roth M. B. (2010) **Hydrogen sulfide increases hypoxia-inducible factor-1 activity independently of von Hippel-Lindau tumor suppressor-1 in C. elegans** *Mol Biol Cell* **21**:212–217 https://doi.org/10.1091/mbc.E09-03-0199

Budde M. W., Roth M. B. (2011) **The response of Caenorhabditis elegans to hydrogen sulfide and hydrogen cyanide** *Genetics* **189**:521–532 https://doi.org/10.1534/genetics.111.129841

Busch K. E., Laurent P., Soltesz Z., Murphy R. J., Faivre O., Hedwig B., de Bono M. (2012) **Tonic signaling from O(2) sensors sets neural circuit activity and behavioral state** *Nat Neurosci* **15**:581–591 https://doi.org/10.1038/nn.3061

Carrillo M. A., Guillermin M. L., Rengarajan S., Okubo R. P., Hallem E. A. (2013) **O-2-Sensing Neurons Control CO2 Response in C. elegans** *Journal of Neuroscience* **33**:9675–9683 https://doi.org/10.1523/Jneurosci.4541-12.2013

Cha'on U., Valmas N., Collins P. J., Reilly P. E., Hammock B. D., Ebert P. R. (2007) **Disruption of iron homeostasis increases phosphine toxicity in Caenorhabditis elegans** *Toxicol Sci* **96**:194–201 https://doi.org/10.1093/toxsci/kfl187

Cheung B. H., Cohen M., Rogers C., Albayram O., de Bono M. (2005) **Experience-dependent modulation of C. elegans behavior by ambient oxygen** *Curr Biol* **15**:905–917 https://doi.org/10.1016/j.cub.2005.04.017

Cooper C. E., Brown G. C. (2008) **The inhibition of mitochondrial cytochrome oxidase by the gases carbon monoxide, nitric oxide, hydrogen cyanide and hydrogen sulfide: chemical mechanism and physiological significance** *J Bioenerg Biomembr* **40**:533–539 https://doi.org/10.1007/s10863-008-9166-6

Couto A., Oda S., Nikolaev V. O., Soltesz Z., de Bono M. (2013) **In vivo genetic dissection of O2-evoked cGMP dynamics in a Caenorhabditis elegans gas sensor** *Proc Natl Acad Sci U S A* **110**:E3301–3310 https://doi.org/10.1073/pnas.1217428110

Dallman P. R. (1986) **Biochemical Basis for the Manifestations of Iron-Deficiency** *Annual Review of Nutrition* **6**:13–40 https://doi.org/10.1146/annurev.nu.06.070186.000305

de Bono M., Bargmann C. I. (1998) **Natural variation in a neuropeptide Y receptor homolog modifies social behavior and food response in C. elegans** *Cell* **94**:679–689 https://doi.org/10.1016/s0092-8674(00)81609-8

Dekker L. V., Mcintyre P., Parker P. J., Retrieved from <GO to ISI>://WOS:A1993LW81900055 (1993) **Mutagenesis of the Regulatory Domain of Rat Protein Kinase-C-Eta - a Molecular-Basis for Restricted Histone Kinase-Activity** *Journal of Biological Chemistry* **268**:19498–19504

Dobin A., Davis C. A., Schlesinger F., Drenkow J., Zaleski C., Jha S., Gingeras T. R. (2013) **STAR: ultrafast universal RNA-seq aligner** *Bioinformatics* **29**:15–21 https://doi.org/10.1093/bioinformatics/bts635

Dokshin G. A., Ghanta K. S., Piscopo K. M., Mello C. C. (2018) **Robust Genome Editing with Short Single-Stranded and Long, Partially Single-Stranded DNA Donors in Caenorhabditis elegans** *Genetics* **210**:781–787 https://doi.org/10.1534/genetics.118.301532

Fawcett E. M., Hoyt J. M., Johnson J. K., Miller D. L. (2015) **Hypoxia disrupts proteostasis in Caenorhabditis elegans** *Aging Cell* **14**:92–101 https://doi.org/10.1111/acel.12301

Ferkey D. M., Sengupta P., L'Etoile N. D. (2021) **Chemosensory signal transduction in Caenorhabditis elegans** *Genetics* **217** https://doi.org/10.1093/genetics/iyab004

Ghanta K. S., Mello C. C. (2020) **Melting dsDNA Donor Molecules Greatly Improves Precision Genome Editing in Caenorhabditis elegans** *Genetics* **216**:643–650 https://doi.org/10.1534/genetics.120.303564

Gourley B. L., Parker S. B., Jones B. J., Zumbrennen K. B., Leibold E. A. (2003) **Cytosolic aconitase and ferritin are regulated by iron in Caenorhabditis elegans** *J Biol Chem* **278**:3227–3234 https://doi.org/10.1074/jbc.M210333200

Gray J. M., Karow D. S., Lu H., Chang A. J., Chang J. S., Ellis R. E., Bargmann C. I. (2004) **Oxygen sensation and social feeding mediated by a C. elegans guanylate cyclase homologue** *Nature* **430**:317–322 https://doi.org/10.1038/nature02714

Hallem E. A., Spencer W. C., McWhirter R. D., Zeller G., Henz S. R., Ratsch G., Ringstad N. (2011) **Receptor-type guanylate cyclase is required for carbon dioxide sensation by Caenorhabditis elegans** *Proc Natl Acad Sci U S A* **108**:254–259 https://doi.org/10.1073/pnas.1017354108

Hallem E. A., Sternberg P. W. (2008) **Acute carbon dioxide avoidance in Caenorhabditis elegans** *Proc Natl Acad Sci U S A* **105**:8038–8043 https://doi.org/10.1073/pnas.0707469105

Hao Y., Yang W., Ren J., Hall Q., Zhang Y., Kaplan J. M. (2018) **Thioredoxin shapes the C. elegans sensory response to Pseudomonas produced nitric oxide** *Elife* **7** https://doi.org/10.7554/eLife.36833

Heiman M. G., Shaham S. (2009) **DEX-1 and DYF-7 establish sensory dendrite length by anchoring dendritic tips during cell migration** *Cell* **137**:344–355 https://doi.org/10.1016/j.cell.2009.01.057

Hildebrandt T. M., Grieshaber M. K. (2008) **Three enzymatic activities catalyze the oxidation of sulfide to thiosulfate in mammalian and invertebrate mitochondria** *FEBS J* **275**:3352–3361 https://doi.org/10.1111/j.1742-4658.2008.06482.x

Hiroki S., Yoshitane H., Mitsui H., Sato H., Umatani C., Kanda S., Iino Y. (2022) **Molecular encoding and synaptic decoding of context during salt chemotaxis in C. elegans** *Nature Communications* **13** https://doi.org/10.1038/s41467-022-30279-7

Horsman J. W., Heinis F. I., Miller D. L. (2019) **A Novel Mechanism To Prevent H2S Toxicity in Caenorhabditis elegans** *Genetics* **213**:481–490 https://doi.org/10.1534/genetics.119.302326

Jackson M. R., Melideo S. L., Jorns M. S. (2012) **Human sulfide:quinone oxidoreductase catalyzes the first step in hydrogen sulfide metabolism and produces a sulfane sulfur metabolite** *Biochemistry* **51**:6804–6815 https://doi.org/10.1021/bi300778t

Kaelin W. G., Ratcliffe P. J. (2008) **Oxygen sensing by metazoans: the central role of the HIF hydroxylase pathway** *Mol Cell* **30**:393–402 https://doi.org/10.1016/j.molcel.2008.04.009

Kelley J. L., Arias-Rodriguez L., Patacsil Martin D., Yee M. C., Bustamante C. D., Tobler M. (2016) **Mechanisms Underlying Adaptation to Life in Hydrogen Sulfide-Rich Environments** *Mol Biol Evol* **33**:1419–1434 https://doi.org/10.1093/molbev/msw020

Khan A. A., Schuler M. M., Prior M. G., Yong S., Coppock R. W., Florence L. Z., Lillie L. E. (1990) **Effects of hydrogen sulfide exposure on lung mitochondrial respiratory chain enzymes in rats** *Toxicol Appl Pharmacol* **103**:482–490 https://doi.org/10.1016/0041-008x(90)90321-k

Kim Y. I., Cho J. H., Yoo O. J., Ahnn J. (2004) **Transcriptional regulation and life-span modulation of cytosolic aconitase and ferritin genes in C.elegans** *J Mol Biol* **342**:421–433 https://doi.org/10.1016/j.jmb.2004.07.036

Kuleshov M. V., Jones M. R., Rouillard A. D., Fernandez N. F., Duan Q. N., Wang Z. C., Ma'ayan A. (2016) **Enrichr: a comprehensive gene set enrichment analysis web server 2016 update** *Nucleic Acids Research* **44**:W90–W97 https://doi.org/10.1093/nar/gkw377

Laurent P., Soltesz Z., Nelson G. M., Chen C., Arellano-Carbajal F., Levy E., de Bono M. (2015) **Decoding a neural circuit controlling global animal state in C. elegans** *Elife* **4** https://doi.org/10.7554/eLife.04241

Lee S. J., Hwang A. B., Kenyon C. (2010) **Inhibition of Respiration Extends C. elegans Life Span via Reactive Oxygen Species that Increase HIF-1 Activity** *Current Biology* **20**:2131–2136 https://doi.org/10.1016/j.cub.2010.10.057

Liao Y., Smyth G. K., Shi W. (2014) **featureCounts: an efficient general purpose program for assigning sequence reads to genomic features** *Bioinformatics* **30**:923–930 https://doi.org/10.1093/bioinformatics/btt656

Liochev S. I. (1996) **The role of iron-sulfur clusters in in vivo hydroxyl radical production** *Free Radical Research* **25**:369–384 https://doi.org/10.3109/10715769609149059

Love M. I., Huber W., Anders S. (2014) **Moderated estimation of fold change and dispersion for RNA-seq data with DESeq2** *Genome Biology* **15** https://doi.org/10.1186/s13059-014-0550-8

Ma D. K., Vozdek R., Bhatla N., Horvitz H. R. (2012) **CYSL-1 interacts with the O2-sensing hydroxylase EGL-9 to promote H2S-modulated hypoxia-induced behavioral plasticity in C. elegans** *Neuron* **73**:925–940 https://doi.org/10.1016/j.neuron.2011.12.037

Macosko E. Z., Pokala N., Feinberg E. H., Chalasani S. H., Butcher R. A., Clardy J., Bargmann C. I. (2009) **A hub-and-spoke circuit drives pheromone attraction and social behaviour in C. elegans** *Nature* **458**:1171–1175 https://doi.org/10.1038/nature07886

Masini A., Salvioli G., Cremonesi P., Botti B., Gallesi D., Ceccarelli D. (1994) **Dietary Iron-Deficiency in the Rat .1. Abnormalities in Energy-Metabolism of the Hepatic Tissue** *Biochimica Et Biophysica Acta-Bioenergetics* **1188**:46–52 https://doi.org/10.1016/0005-2728(94)90020-5

Masini A., Trenti T., Caramazza I., Predieri G., Gallesi D., Ceccarelli D. (1994) **Dietary Iron-Deficiency in the Rat .2. Recovery from Energy-Metabolism Derangement of the Hepatic Tissue by Iron Therapy** *Biochimica Et Biophysica Acta-Bioenergetics* **1188**:53–57 https://doi.org/10.1016/0005-2728(94)90021-3

Mathew N. D., Schlipalius D. I., Ebert P. R. (2011) **Sulfurous gases as biological messengers and toxins: comparative genetics of their metabolism in model organisms** *J Toxicol* **2011** https://doi.org/10.1155/2011/394970

Melo J. A., Ruvkun G. (2012) **Inactivation of Conserved C. elegans Genes Engages Pathogen- and Xenobiotic-Associated Defenses** *Cell* **149**:452–466 https://doi.org/10.1016/j.cell.2012.02.050

Miller D. L., Budde M. W., Roth M. B. (2011) **HIF-1 and SKN-1 Coordinate the Transcriptional Response to Hydrogen Sulfide in Caenorhabditis elegans** *PLoS One* **6** https://doi.org/10.1371/journal.pone.0025476

Miller D. L., Budde M. W., Roth M. B. (2011) **HIF-1 and SKN-1 coordinate the transcriptional response to hydrogen sulfide in Caenorhabditis elegans** *PLoS One* **6** https://doi.org/10.1371/journal.pone.0025476

Miller D. L., Roth M. B. (2007) **Hydrogen sulfide increases thermotolerance and lifespan in Caenorhabditis elegans** *Proc Natl Acad Sci U S A* **104**:20618–20622 https://doi.org/10.1073/pnas.0710191104

Mishanina A. V., Libiad M., Banerjee R. (2015) **Biogenesis of reactive sulfur species for signaling by hydrogen sulfide oxidation pathways** *Nature Chemical Biology* **11**:457–464 https://doi.org/10.1038/nchembio.1834

Murakami M., Koga M., Ohshima Y. (2001) **DAF-7/TGF-beta expression required for the normal larval development in C-elegans is controlled by a presumed guanylyl cyclase DAF-11** *Mechanisms of Development* **109**:27–35 https://doi.org/10.1016/S0925-4773(01)00507-X

Murayama T., Toh Y., Ohshima Y., Koga M. (2005) **The dyf-3 gene encodes a novel protein required for sensory cilium formation in Caenorhabditis elegans** *J Mol Biol* **346**:677–687 https://doi.org/10.1016/j.jmb.2004.12.005

Myllyharju J., Kivirikko K. I. (1997) **Characterization of the iron- and 2-oxoglutarate-binding sites of human prolyl 4-hydroxylase** *Embo Journal* **16**:1173–1180 https://doi.org/10.1093/emboj/16.6.1173

Nicholls P., Kim J. K. (1982) **Sulfide as an Inhibitor and Electron-Donor for the Cytochrome-C Oxidase System** *Canadian Journal of Biochemistry* **60**:613–623 https://doi.org/10.1139/o82-076

Nicholls P., Kim J. K. (1982) **Sulphide as an inhibitor and electron donor for the cytochrome c oxidase system** *Can J Biochem* **60**:613–623 https://doi.org/10.1139/o82-076

Niu W., Lu Z. J., Zhong M., Sarov M., Murray J. I., Brdlik C. M., Reinke V. (2011) **Diverse transcription factor binding features revealed by genome-wide ChIP-seq in C. elegans** *Genome Research* **21**:245–254 https://doi.org/10.1101/gr.114587.110

Olson K. R., Straub K. D. (2016) **The Role of Hydrogen Sulfide in Evolution and the Evolution of Hydrogen Sulfide in Metabolism and Signaling** *Physiology (Bethesda)* **31**:60–72 https://doi.org/10.1152/physiol.00024.2015

Pekec T., Lewandowski J., Komur A. A., Sobanska D., Guo Y., Switonska-Kurkowska K., Ciosk R. (2022) **Ferritin-mediated iron detoxification promotes hypothermia survival in Caenorhabditis elegans and murine neurons** *Nat Commun* **13** https://doi.org/10.1038/s41467-022-32500-z

Persson A., Gross E., Laurent P., Busch K. E., Bretes H., de Bono M. (2009) **Natural variation in a neural globin tunes oxygen sensing in wild Caenorhabditis elegans** *Nature* **458**:1030–1033 https://doi.org/10.1038/nature07820

Pfenninger M., Lerp H., Tobler M., Passow C., Kelley J. L., Funke E., Plath M. (2014) **Parallel evolution of cox genes in H2S-tolerant fish as key adaptation to a toxic environment** *Nat Commun* **5** https://doi.org/10.1038/ncomms4873

Philipp T. M., Gong W., Kohnlein K., Ohse V. A., Muller F. I., Priebs J., Klotz L. O. (2022) **SEMO-1, a novel methanethiol oxidase in Caenorhabditis elegans, is a pro-aging factor conferring selective stress resistance** *Biofactors* **48**:699–706 https://doi.org/10.1002/biof.1836

Qabazard B., Li L., Gruber J., Peh M. T., Ng L. F., Kumar S. D., Moore P. K. (2014) **Hydrogen sulfide is an endogenous regulator of aging in Caenorhabditis elegans** *Antioxid Redox Signal* **20**:2621–2630 https://doi.org/10.1089/ars.2013.5448

Rajan M., Anderson C. P., Rindler P. M., Romney S. J., Ferreira Dos Santos M. C., Gertz J., Leibold E. A. (2019) **NHR-14 loss of function couples intestinal iron uptake with innate immunity in C. elegans through PQM-1 signaling** *Elife* **8** https://doi.org/10.7554/eLife.44674

Read A. D., Bentley R. E. T., Archer S. L., Dunham-Snary K. J. (2021) **Mitochondrial iron-sulfur clusters: Structure, function, and an emerging role in vascular biology** *Redox Biology* **47** https://doi.org/10.1016/j.redox.2021.102164

Rodriguez-Kabana R., Jordan J. W., Hollis J. P. (1965) **Nematodes: Biological Control in Rice Fields: Role of Hydrogen Sulfide** *Science* **148**:524–526 https://doi.org/10.1126/science.148.3669.524

Romney S. J., Newman B. S., Thacker C., Leibold E. A. (2011) **HIF-1 regulates iron homeostasis in Caenorhabditis elegans by activation and inhibition of genes involved in iron uptake and storage** *PLoS Genet* **7** https://doi.org/10.1371/journal.pgen.1002394

Salvanes A. G. V., Utne-Palm A. C., Currie B., Braithwaite V. A. (2011) **Behavioural and physiological adaptations of the bearded goby, a key fish species of the extreme environment of the northern Benguela upwelling** *Marine Ecology Progress Series* **425**:193–202 https://doi.org/10.3354/meps08998

Semenza G. L. (2010) **Defining the role of hypoxia-inducible factor 1 in cancer biology and therapeutics** *Oncogene* **29**:625–634 https://doi.org/10.1038/onc.2009.441

Shefa U., Kim M. S., Jeong N. Y., Jung J. (2018) **Antioxidant and Cell-Signaling Functions of Hydrogen Sulfide in the Central Nervous System** *Oxidative Medicine and Cellular Longevity* **2018** https://doi.org/10.1155/2018/1873962

Siegert I., Schodel J., Nairz M., Schatz V., Dettmer K., Dick C., Jantsch J. (2015) **Ferritin-Mediated Iron Sequestration Stabilizes Hypoxia-Inducible Factor-1 alpha upon LPS Activation in the Presence of Ample Oxygen** *Cell Reports* **13**:2048–2055 https://doi.org/10.1016/j.celrep.2015.11.005

Starich T. A., Herman R. K., Kari C. K., Yeh W. H., Schackwitz W. S., Schuyler M. W., Riddle D. L. (1995) **Mutations affecting the chemosensory neurons of Caenorhabditis elegans** *Genetics* **139**:171–188 https://doi.org/10.1093/genetics/139.1.171

Sunda W., Kieber D. J., Kiene R. P., Huntsman S. (2002) **An antioxidant function for DMSP and DMS in marine algae** *Nature* **418**:317–320 https://doi.org/10.1038/nature00851

Swoboda P., Adler H. T., Thomas J. H. (2000) **The RFX-type transcription factor DAF-19 regulates sensory neuron cilium formation in C. elegans** *Mol Cell* **5**:411–421 https://doi.org/10.1016/s1097-2765(00)80436-0

Vora M., Pyonteck S. M., Popovitchenko T., Matlack T. L., Prashar A., Kane N. S., Rongo C. (2022) **The hypoxia response pathway promotes PEP carboxykinase and gluconeogenesis in C. elegans** *Nature Communications* **13** https://doi.org/10.1038/s41467-022-33849-x

Walter P. B., Knutson M. D., Paler-Martinez A., Lee S., Xu Y., Viteri F. E., Ames B. N. (2002) **Iron deficiency and iron excess damage mitochondria and mitochondrial DNA in rats** *Proceedings of the National Academy of Sciences of the United States of America* **99**:2264–2269 https://doi.org/10.1073/pnas.261708798

Xu X. M., Moller S. G. (2011) **Iron-Sulfur Clusters: Biogenesis, Molecular Mechanisms, and Their Functional Significance** *Antioxidants & Redox Signaling* **15**:271–307 https://doi.org/10.1089/ars.2010.3259

Zhao L., Fenk L. A., Nilsson L., Amin-Wetzel N. P., Ramirez-Suarez N. J., de Bono M., Chen C. (2022) **ROS and cGMP signaling modulate persistent escape from hypoxia in Caenorhabditis elegans** *PLoS Biol* **20** https://doi.org/10.1371/journal.pbio.3001684

Zimmer M., Gray J. M., Pokala N., Chang A. J., Karow D. S., Marletta M. A., Bargmann C. I. (2009) **Neurons detect increases and decreases in oxygen levels using distinct guanylate cyclases** *Neuron* **61**:865–879 https://doi.org/10.1016/j.neuron.2009.02.013

Article and author information

Longjun Pu
Department of Molecular Biology, Umeå University, Umeå, Sweden, Umeå Centre for Molecular Medicine, Umeå University, Umeå, Sweden, Wallenberg Centre for Molecular Medicine, Umeå University, Umeå, Sweden

Lina Zhao
Department of Molecular Biology, Umeå University, Umeå, Sweden, Umeå Centre for Molecular Medicine, Umeå University, Umeå, Sweden, Wallenberg Centre for Molecular Medicine, Umeå University, Umeå, Sweden

Jing Wang
Department of Molecular Biology, Umeå University, Umeå, Sweden, Umeå Centre for Molecular Medicine, Umeå University, Umeå, Sweden, Wallenberg Centre for Molecular Medicine, Umeå University, Umeå, Sweden

Johan Henriksson
Department of Molecular Biology, Umeå University, Umeå, Sweden, The Laboratory for Molecular Infection Medicine Sweden (MIMS), Umeå University, Umeå, Sweden, Integrated Science Lab (Icelab), Umeå University, Umeå, Sweden
ORCID iD: 0000-0002-7745-2844

Patrick Laurent
Laboratory of Neurophysiology, ULB Neuroscience Institute (UNI), Université Libre de Bruxelles (ULB), Belgium

Changchun Chen
Department of Molecular Biology, Umeå University, Umeå, Sweden, Umeå Centre for Molecular Medicine, Umeå University, Umeå, Sweden, Wallenberg Centre for Molecular Medicine, Umeå University, Umeå, Sweden
For correspondence: changchun.chen@umu.se
ORCID iD: 0000-0003-2233-8996

Copyright

Editors

Reviewing Editor
Douglas Portman
University of Rochester, Rochester, United States of America

Senior Editor
Albert Cardona
University of Cambridge, Cambridge, United Kingdom

Reviewer #1 (Public Review):

Summary:
This paper sets out to achieve a deeper understanding of the effects of hydrogen sulfide on C. elegans behavior and physiology, with a focus on behavior, detection mechanism(s), physiological responses, and detoxification mechanisms.

Strengths:
The paper takes full advantage of the experimental tractability of C. elegans, with thorough, well-designed genetic analyses.
Some evidence suggests that H2S may be directly detected by the ASJ sensory neurons.
The paper provides interesting and convincing evidence for complex interactions between responses to different gaseous stimuli, particularly an antagonistic role between H2S and O2 detection/response.
Intriguing roles for mitochondria and iron homeostasis are identified, opening the door to future studies to better understand the roles of these components and processes.

Weaknesses:
The claim that worms' behavioral responses to H2S are mediated by direct detection is incompletely supported. While a role for the chemosensory neuron ASJ is implicated, it remains unclear whether this reflects direct detection. Other possibilities, including indirect effects of ASJ and the guanylyl cyclase daf-11 on O2 responses, are also consistent with the authors' data.

The role of H2S-mediated damage in behavioral responses, particularly when detoxification pathways are disrupted, remains unclear.

The findings of the paper are somewhat disjointed, such that a clear picture of the relationships between H2S detection, detoxification mechanisms, mitochondria, and iron does not emerge from these studies. Most importantly, the relative roles of H2S detection and integration, vs. general and acute mitochondrial crisis, in generating behavioral responses are not convincingly resolved.

- https://doi.org/10.7554/eLife.92964.1.sa2

Reviewer #2 (Public Review):

Summary:

H2S is a gas that is toxic to many animals and causes avoidance in animals such as C. elegans. The authors show that H2S increases the frequency of turning and the speed of locomotion. The response was shown to be modulated by a number of neurons and signaling pathways as well as by ambient oxygen concentrations. The long-term adaptation involved gene expression changes that may be related to iron homeostasis as well as the homeostasis of mitochondria.

Strengths:

Overall, the authors provide many pieces that will be important for solving how H2S signals through neuronal circuits to change gene expression and physiological programs. The experiments rely mostly on a behavioral assay that measures the increase of locomotion speed upon exposure to H2S. This assay is then combined with manipulations of environmental factors, different wild-type strains, and mutants. The mutants analyzed were obtained as candidates from the literature and from transcriptional profiling that the authors carried out in worms that were exposed to H2S. These studies imply several genetic signaling pathways, some neurons, and metabolism-related factors in the response to H2S. Hence the data provided should be useful for the field.

Weaknesses:

On the other hand, many important aspects of the underlying mechanisms remain unsolved and the reader is left with many loose ends. For example, it is not clear how H2S is actually sensed, how sensory neurons are activated and signal to downstream circuits, and what the role of ciliated and RMG neurons is in this circuit. It remains unclear how signals lead to gene expression and physiological changes such as metabolic rewiring. Solving all this would clearly be beyond the scope of a single manuscript. Yet, the manuscript also does not focus on understanding one of these central aspects and rather is all over the place, which makes it harder to understand for readouts that are not in this core field. Multiple additional methods and approaches exist to dig deeper into these mechanisms in the future, such as neuronal calcium imaging, optogenetics, and metabolic analysis. To generate a story that will be interesting to a broad readership substantial additional experimentation would be required. Further, in the current manuscript, it is often difficult to understand the rationales of the experiments, why they were carried out, and how to place them into a context. This could be improved in terms of documentation, narration/explanation, and visualization.

- https://doi.org/10.7554/eLife.92964.1.sa1

Reviewer #3 (Public Review):

Summary:
The manuscript explores the behavioral responses of C. elegans to hydrogen sulfide, which is known to exert remarkable effects on animal physiology in a range of contexts. The possibility of genetic and precise neuronal dissection of responses to H2S motivates the study of responses in C. elegans. The manuscript is well-written in communicating the complex physiology around C. elegans behavioral responses to H2S and in appropriately citing prior and related relevant work.

There are three parts to the manuscript.

In the first, an immediate behavioral response-increased locomotory rate-upon exposure to H2S is characterized. The experimental conditions are critical, and data are obtained from exposure of animals to 150ppm H2S at 7% O2. The authors provide evidence that this is a chemosensory response to H2S, showing a requirement for genes encoding components of the cilia apparatus and implicating a role for tax-4 and daf-11. Neuron-specific rescue in the ASJ neurons suggests the ASJ neurons contribute to the response to H2S. One caveat is that previous work has shown that the dauer-constitutive phenotype of daf-11 mutants can be suppressed by ASJ ablation, suggesting that there may be pervasive changes in animal nervous system signaling that are ASJ-dependent in daf-11 mutants, which may indirectly alter chemosensory responses to H2S. More direct methods to assess whether ASJ senses H2S, e.g. using calcium imaging, would better assess a direct role for the ASJ neurons in a behavioral response to H2S. The authors also point out interesting parallels between the response to H2S and CO2 though provide some genetic data separating the two responses. Importantly, the authors note that when aerotaxis (O2-sensing and movement) in the

presence of bacterial food is intact, as in npr-1 215F animals, the response to H2S is abrogated. Mutation in gcy-35 in the npr-1 215F background restores the H2S chemosensory response.

There is a second part of the paper that conducts transcriptional profiling of the response to H2S that corroborates and extends prior work in this area.

The final part of the paper is the most intriguing, but for me, also the most problematic. The authors examine how H2S-evoked locomotory behavioral responses are affected in mutants defective in the stress and detoxification response to H2S, most notably hif-1. Prior genetic studies have established the pathways leading to HIF-1 activation/stabilization, as well as potential downstream mechanisms. The authors conduct logical genetic analysis to complement studies of the hif-1 mutant and in part motivated by their transcriptional profiling studies, examine the role of iron sequestration/free iron in the locomotory response to H2S, and further speculate on how the behavior of mutants defective in mitochondrial function might be affected by exposure to H2S.

In some regard, this part of the manuscript is interesting because the analysis begins to connect how the behavior of an animal to a toxic compound is affected by mutations that affect sensitivity to the toxic compound. However, what is unclear is what is being studied at this point. In the context, of noting that H2S at 150ppm is known to be lethal, its addition to mutants clearly sensitized to its effects would be anticipated to have pervasive effects on animal physiology and nervous system function. The authors note that the continued increased locomotion of wild-type animals upon H2S exposure might be due to the byproducts of detoxification or the detrimental effects of H2S. The latter explanation seems much more likely, in which case what one may be observing is the effects of general animal sickness, or even a bit more specifically, neuronal dysfunction in the presence of a toxic compound, on locomotion. As such, what is unclear is what conclusions can be taken away from this part of the work.

Strengths:
1. Characterization of a motor behavior response to H2S
2. Transcriptional profiling of the response to H2S corroborating prior work.

Weaknesses:
Unclear significance and experimental challenges regarding the study of locomotory responses to animals sensitized to the toxic effects of H2S under exposure to H2S.

- https://doi.org/10.7554/eLife.92964.1.sa0